Alma Mater Studiorum – Università di Bologna

DOTTORATO DI RICERCA IN

SCIENZE CARDIO NEFRO TORACICHE

Ciclo XXXIII

Settore Concorsuale: MED/14 - Endocrinologia, Nefrologia e scienze dell'alimentazione e del benessere

Settore Scientifico Disciplinare: Nefrologia

PROTECTIVE EFFECTS OF PODOCYTE-EXPRESSED DECAY ACCELERATING FACTOR IN FOCAL AND SEGMENTAL GLOMERULOSCLEROSIS

Presentata da: **Dr. Andrea Angeletti**

Coordinatore Dottorato
Prof. Gaetano Domenico Gargiulo

Supervisore
Prof. Gaetano La Manna

Esame finale anno 2021

ABSTRACT

Kidney glomerulosclerosis commonly progresses to end-stage kidney failure, but pathogenic mechanisms are still poorly understood. Here, we show that podocyte expression of decay-accelerating factor (DAF/CD55), a complement C3 convertase regulator, crucially controls disease in murine models of adriamycin (ADR)-induced focal and segmental glomerulosclerosis (FSGS) and streptozotocin (STZ)-induced diabetic glomerulosclerosis. ADR induces enzymatic cleavage of DAF from podocyte surfaces, leading to complement activation. C3 deficiency or prevention of C3a receptor (C3aR) signaling abrogates disease despite DAF deficiency, confirming complement dependence. Mechanistic studies show that C3a/C3aR ligations on podocytes initiate an autocrine IL-1β/IL-1R1 signaling loop that reduces nephrin expression, causing actin cytoskeleton rearrangement. Uncoupling IL-1β/IL-1R1 signaling prevents disease, providing a causal link. Glomeruli of patients with FSGS lack DAF and stain positive for C3d, and urinary C3a positively correlates with the degree of proteinuria. Together, our data indicate that the development and progression of glomerulosclerosis involve loss of podocyte DAF, triggering local, complement-dependent, IL-1β-induced podocyte injury, potentially identifying new therapeutic targets.

INTRODUCTION

Primary focal and segmental glomerulosclerosis (FSGS) represents one of the leading causes of idiopathic nephrotic syndrome in adults and child [1]. The treatment of choice is represented by steroid, achieving a sustained remission in less than 50% of affected subjects and, among who do not achieve remission, progression to end stage renal disease (ESRD) is reported for a consistent part [2]. Considering the limited therapeutic efficacy and the toxicity of these drugs, alternative interventions are needed for improved therapeutical approaches, ideally derived from new knowledge of disease pathogenesis [3].

While the discovery of genetic variants [4] that predispose to development of FSGS has provided some mechanistic insight into the pathogenesis of disease in a subset of patients, podocyte injury and depletion represents the key pathogenic features of disease progression, as suggested by evidence derived from multiple experimental models [5-7]. The driving forces underlying podocyte injury remain inadequately understood, therefore the development of novel therapeutics results still limited [7].

The complement cascade, traditionally considered a constituent of innate immunity required for host defense against pathogens, is now recognized as a crucial pathogenic mediator of various kidney diseases [8, 9]. Complement components produced by the liver and circulating in the plasma undergo activation through the classical and/or mannose-binding lectin pathways to mediate autoantibody-initiated glomerulonephritides (GN) [10]. The alternative pathway of complement activation has been implicated in

non-antibody-mediated models of GN including human and murine C3 nephropathies [11-13]. While selected studies in murine models that mimic features of human FSGS have been associated with complement deposition, mechanisms linking complement to podocyte injury and FSGS remain poorly understood [10].

Decay accelerating factor (DAF, CD55), a cell surface expressed, glycophosphatidyl inositol (GPI)-anchored protein, regulates complement activation at the C3/C4 convertase steps. A previous report indicated that, in mice with FSGS induced by injection of sheep antibodies against mouse podocytes, the absence of DAF in T cells is correlated with worsen of disease severity, but mechanisms have not been elucidated [14]. That DAF is highly expressed on podocytes is well known, therefore we tested the hypothesis that DAF locally restrains complement activation and as a consequence, its downregulation leads to complement-mediated podocyte injury that results in FSGS.

MATERIALS AND METHODS

Mice and procedures

Wild-type (WT) BALB/c and C57BL/6J (B6) mice were purchased from The Jackson Laboratory (Bar Harbor, MA). To generate $DAF^{fl/fl}$ mice, we obtained embrionic stem (ES) cells from European Conditional Mouse Mutagenesis Program (EUCOMM). The ES cells were injected into pseudopregnant B6 mice (The Jackson Laboratory) by standard techniques at the mouse genetics core facility at Icahn School of Medicine at Mount Sinai. Founders were validated by genotyping. We then crossed them to a flp/flp mouse (from Jax) to remove the neo cassette and then backcrossed to B6 and crossed with B6 mice expressing the Podocin-Cre or CD11c-Cre (The Jackson Laboratory).

Animal experiments were performed with the approval of the Institutional Animal Care and Use Committee of Icahn School of Medicine at Mount Sinai, New York.

Male and female mice (age 8-12 weeks), with a body weight of 20 to 25 g, were treated with a single retro-orbital injection of ADR (doxorubicin HCl, Ben Venue Laboratories, Bedford, OH), at the dose of 10 mg/kg for BALB/c or 20 mg/kg for B6 mice. C3aR-A (SB290157, Sigma-Aldrich, MO) or vehicle control was administered through subcutaneous pumps (micro-osmotic pump, model 1004, Alzet, CA) at the dose of 1 mg/kg/die (powder dissolved in PBS and 10% DMSO) for 28 days. Rat anti-mouse IL-1β mAb (InVivoMab, B122, BioXCell, NH) or isotype control (InVivoMab polyclonal Armenian hamster IgG, BioXCell) was administed i.p. at the dose of 50 μg/mice twice a week for 6 weeks [15].

Renal histology

To obtain kidneys, mice were anesthetized with i.p. injection of 100 µl of a solution made of sterile ketamine (16 mg/ml) and xylazine (7 mg/ml) in phosphate buffered saline (PBS, Gibco, CA) and trans-cardially perfused with periodate-lysin-paraformaldehyde fixate at 4% in PBS. Kidneys were harvested and frozen in Optimal Cutting Temperature compound (Tissue-Tek O.C.T., Sakura, CA) or paraffin-embedded. In selected experiments, one kidney was removed and clamped before periodate-lysin-paraformaldehyde fixation of the other kidney.

Light microscopy

Paraffin-embedded kidney sections (3 µm) were stained with Periodic acid–Schiff (PAS). Histological scoring was performed in a blinded manner by a renal pathologist. The extent of segmental and global glomerular sclerosis was assessed by examining all glomeruli on a kidney cross-section, and calculating the percent involved as previously described [16].

Immunofluorescence

O.C.T.-preserved cryosections (5 µm thick) were washed with PBS for 5 minutes, then left for 30 to 60 min at room temperature with blocking solution containing PBS, 2% bovine serum albumin, 2% fetal bovine serum, and 0.2% fish gelatin. Affinipure fab fragment goat anti mouse IgG (Jackson ImmunoResearch, PA) was subsequently applied for 3 hours, followed by incubation at 4°C overnight or at room temperature for 1 hour with specific primary antibodies (see table below). Sections were then washed

and incubated with the appropriate secondary antibody for 45 or 60 minutes at room temperature: anti-mouse IgG antibody conjugated with Alexa Fluor 594 (1:200; Thermo Fisher Scientific, MA), anti-hamster IgG antibody conjugated with Alexa Fluor 488 (1:200; Thermo Fisher Scientific), and anti-rat IgG antibody conjugated with Alexa Fluor 568 (1:500; Life Technologies, CA), anti-rabbit IgG antibody conjugated with Alexa Fluor 594 (1:500; Life Technologies), anti-mouse IgG antibody conjugated with Alexa Fluor 594 (1:500; Jackson ImmunoResearch), anti-goat IgG antibody conjugated with Alexa Fluor 594 (1:500; Life Technologies) were used. Nuclei were counterstained with DAPI mounting media (ProLong Gold antifade reagent with DAPI, P36931, Invitrogen, CA).

Antibodies expression was estimated by constructing a contour mask on the bright-field image. Software ImageJ was used to quantify DAF and C3b staining intensity.

List of antibodies and assay-specific concentrations

Antibody	**Reactive Species**	**Company**	**Catalogue #**	**Dilution**
Synaptopodin	mouse	Fitzgerald	10R-S125a	IF 1:5
Podocin (NPHS2)	mouse	Sigma-Aldrich	P0372	IF 1:50
CD55	mouse	BioLegend	(Riko-5) 131802	IF 1:50
CD55	human	Santa Cruz Biotechnology	sc-51733	IF 1:50 WB 1:100
C1q	rat	Abcam	ab11861	IF 1:50

C4b	rabbit	Abcam	ab181241	IF 1:50
CD59 (FITC)	mouse	LSBio	LS-C210253	IF 1:50
Claudin-1	human	Thermo Fisher	51-9000	IF 1:25
C3b	mouse, human	Hycult Biotech	HM1065	IF 1:50
C3b (FITC)	mouse	Cappel		IF 1:100
Phalloidin (Alexa fluor 568)	human	Invitrogen	A12380	IF 1:1,000
F-actin (FITC)	human?	Life Technologies	r37122	IF 1 drop/ml
NPHS1	human, mouse	Abcam	ab136894	WB 1:1,000
GPI-PLD	human	Abcam	Ab210753	WB 1:1,000
B-actin	human	GeneTex Sigma-Aldrich	GTX109639 A3854	WB 1:10,000
C3aR	mouse	Origene	BP4002	IF 1:100

Renal ultrastructural analysis

Fresh kidneys underwent primary fixation with 2% glutaraldehyde in PBS. They were then post-fixed in 1% osmium tetroxide for 1 hour and dehydrated in 50%,70%, 90%, 95%, 100%, ethanol and propylene oxide for 10 minutes each. Samples were further infiltrated with epoxy resin mixture. Ultra-thin sections were collected on copper grids, and sections were stained using 10% uranyl acetate in 50% methanol and modified Sato lead stain. A Morgagni 268 electron microscope was used for picture acquisition (Pathology Laboratory, Columbia University, New York, NY). Total glomerular capillary surface area with foot process effacement were evaluated by ultrastructural

analysis (>8 glomeruli/mouse) and graded on a percentage quantification, as previously reported [17].

Urine Albumin and Creatinine

Urine spot samples were collected from individual mice before treatment and at weekly intervals until sacrifice. Urine creatinine was quantified using commercial kits from Cayman Chemical (Ann Arbor, MI). Urine albumin was determined using a commercial assay from Bethyl Laboratory Inc. (Houston, TX). Urine albumin excretion was expressed as the ratio of urine albumin to creatinine.

Cell Culture

Human immortalized podocytes (hiPod) were cultured as described by Saleem et al. [18]. Re-differentiation of hiPod was performed by thermoshifting to 37°C for up to 15 days.

As indicated in the text, some experiments were repeated in human kidney progenitor cells derived from amniotic fluid (hAKPC) that were isolated and characterized as previously described [19]. Briefly, hAKPC positively selected for OB-cadherin, CD24 and podocalyxin were expanded and differentiated into podocytes (hAKPC-P) by culturing on collagen I (Corning, NY)-coated plates in VRADD media: RPMI-1640 (Gibco) supplemented with 10% FBS (Gibco), 1% antibiotic (Gibco), 1,25(OH)2D3 [100 nM, cholecalciferol] (Sigma-Aldrich), all trans retinoic acid (ATRA) [1μM] dexamethasone [100nM] (Sigma-Aldrich), for up to 30 days.

Twenty-four hour in vitro experiments were established for hAKPC-P and hiPod (in quadruplicates). Cells were initially cultured for 24 hours at a concentration of 200,000 cells per 12-well collagen I coated plates, then incubated for 2 hours in RPMI-1640 supplemented with 0.2% FBS and 1% antibiotic. After 2 hours, the following groups were established: cells + goat IgG (0.5 µg/mL, R&D Systems, MN), C3a (50 nM) + goat IgG, or C3a + anti-IL-1ß antibody (0.5 µg/mL, Gibco), and incubated for 30 minutes or 24 hours. Protein lysates were collected and stored in -80°C until analysis.

Twelve-well chamber slides were also created for immunofluoresecne studies with the following culture conditions: 1) vehicle, C3a (50 nM), or C3a + C3aR-A (50 nM), 2) goat IgG (0.5 µg/mL, R&D Systems), IL-1ß + goat IgG, IL-1ß + anti-IL-1ß Ab (0.5 µg/mL, Gibco), C3a (50 nM), or C3a + anti-IL-1ß Ab (0.5 µg/mL, Gibco), and 3) vehicle, ADR (0.3 µg/ml) (Pfizer, NY), vehicle + PLAD inhibitor (1 µM, 1-10 phenantroline, Sigma-Aldrich), or ADR + PLAD inhibitor.

Real-time quantitative reverse transcription PCR

RNA was prepared from 0.5 cm of the mouse kidneys or from cultured podocytes using Trizol (Invitrogen). cDNA was synthesized using reverse transcription reagent (Applied Biosystems). Real-time PCR assays using the TaqMan universal PCR Master Mix and primer sets for human and/or mouse *DAF* (Hs00892618_m1; Mm00438377_m1), *PLAD* (Hs00946499_m1; Mm01289339_m1), *IL1B (Hs01555410_m1), Rn18S* (Hs99999901_s1; Mm03928990_g1), and *GAPDH* (Hs02786624_g1; Mm99999915_g1) genes were purchased from Thermo

Fisher. PCR was performed on an Applied Biosystems 7500 Fast system. All experiments were performed at least in triplicate, and gene expression was normalized to housekeeping gene *18s* or *GAPDH*.

Immunofluorescence studies in vitro

Immunofluorescence staining was performed on chamber slides of representative cell types (hAKPC-P and hiPod) following 20 minutes fixation by 4% paraformaldehyde (Santa Cruz Biotechnology, Dallas, TX) and serial washes with PBS after 24 hours incubation with components. Wells of interest were prepared for staining by blocking with 5% bovine serum albumin (Jackson ImmunoResearch) in PBS for 30 minutes. Damage to podocytes was assessed by 1 hour incubation at room temperature with F-actin (1 drop: 1000 µl, Life Technologies) followed by DAPI mounting (Vector Laboratories, CA). DAF expression was assessed by staining cells with anti-DAF Ab (see table above) at 4˚C overnight, followed by washing and staining with secondary antibody (anti mouse Alexa Fluor 488 Thermo Fisher Scientific, 1:200 in blocking solution) for 1 hour at room temperature. Cells were then permeabilized with 0.1% Triton X-100/PBS (15 minutes) and stained for F-actin (Phalloidin, Alexa fluor 568, Invitrogen, 1:1000). Nuclei were counterstained with DAPI mounting media (ProLong Gold antifade reagent with DAPI, Invitrogen).

Cells were visualized with a Leica DM5500 B Microscope System. Minimum of 5 20× immunofluorescent microscopic images (Leica DM5500 B Microscope System) per ex-

perimental group were counted for cytoskeletal rearrangement expression. ImageJ software (NIH) was used to determine cell count.

In each field, cells were segmented based on the actin signaling, and the intensity of DAF normalized to the intensity of actin pixel-by-pixel. The mean fluorescence intensity (MFI) of the DAF signal was then calculated for all the pixels in the cell.

Western Blot Analysis

Total protein from was extracted from in vitro podocyte cultures, by initially washing cells with PBS, then scraping the cells with a plastic 1.8 cm blade cell scraper (Falcon Cell Scraper, Thermo Fisher Scientific) in radioimmunoprecipitation assay RIPA lysis buffer (Santa Cruz Biotechnology) or 1% SDS lysis buffer (Millipore Sigma, Burlington, MA) containing a protease inhibitor cocktail (Thermo Fisher Scientific). Protein lysates were centrifuged at 13500 rpm, 4°C for 15 minutes to obtain the protein suspension. The supernatants were then collected and protein extracts were separated on 4%–20% pre-cast Protean TGX gels (Bio-Rad, CA) followed by transfer onto 0.2 μm polyvinylidene fluoride (PVDF) membranes (Bio-Rad) using the Trans-blot Turbo transfer system (Bio-Rad). Membranes were soaked in methanol 100% for 5 minutes, quickly rinsed in 0.1% tween 20 (Sigma-Aldrich), 1X Tris-buffered saline buffer (TBS-T). Blocking was performed in 5% non-fat dry milk (Santa Cruz Biotechnology) in TBS-T buffer for 1 hour at room temperature, followed by primary antibody (1:1000 NPHS1, Abcam, Cambridge, UK) or incubation (in 2.5% milk solution) overnight at 4°C in rocking conditions. Following washes in TBS-T buffer (10 minutes for 3 times), membranes were

blotted with host-specific horseradish peroxidase (HRP)-conjugated secondary antibodies diluted in 2.5% skim milk (in TBS-T) at room temperature for 30 minutes. Signal was detected by using the SuperSignal West Femto substrate (Thermo Fisher Scientific) and impressed on Amersham Hyperfilm ECL (GE Healthcare, IL). Densitometry was performed on images using ImageJ software. Protein analysis of podocyte culture supernatants was performed after concentrating 10 ml of cell culture supernantant in an Amicon Ultracentrifugal filter unit (Millipore Sigma) per manufacturer's instructions. 30 µl of concentrated supernatant were run on Bolt Bis-Tris 4%-12% pre-cast gel (Thermo Fisher Scientific), transferred and blocked as described above. Membranes were probed with anti-DAF (1:100, Santa Cruz Biotechnology) and then with secondary antibodies, as described above. Membranes were developed on an Odyssey Fc Imaging system (Li-Cor, Lincoln, NE) and quantified using ImageStudio software (Li-Cor).

Cytokine Analysis

Media from hiPod cultured for 24 hours without and with C3a (50 nM), or C3a (50 nM) + C3aR antagonist (50 nM) was collected and stored in the -80°C until used to evaluate cytokine expression in accords to manufacturer protocols. To perform cytokine measurements, samples were thawed and protein expression profiles were obtained using a Proteome Profiler Human XL Cytokine Array Kit (R&D Systems), a membrane-based sandwich immunoassay that measures 102 human cytokines and growth factors simultaneously, following manufacturer protocols. Briefly, samples were incubated overnight with the nitrocellulose membranes after a blocking step, washed to remove nonspecific proteins, and biotin-labeled detection antibodies were added. The cy-

tokine-antibody-biotin complexes were visualized using chemiluminescent detection reagents. Average chemiluminescent intensity was obtained by measuring pixel density.

Patients

We studied paraffin-embedded renal tissues of 3 patients with FSGS from the archives of the Unit of Nephrology, Dialysis and Kidney Transplant St. Orsola Hospital (Bologna, Italy). Demographic and clinical parameters (proteinuria and serum creatinine levels, and glomerular filtration rate estimated by the "Chronic Kidney Disease Epidemiology Collaboration" equation, CKD-Epi) at the time of renal biopsy were retrieved from the hospital database.

We analyzed 70 frozen urine supernatants from FSGS patients obtained at the Unit of Nephrology, Dialysis and Kidney Transplant St. Orsola Hospital, Bologna, Italy.

All experimental protocols involving human subjects and requiring informed consent are carried out in accordance with the Declaration of Helsinki and good clinical practice guidelines, and approved by the Institutional Review Board (IRB) of the Clinical Research Center of the St. Orsola Hospital (IRB: 420/2018/Oss/AOUBo).

As control, we used renal specimens of deceased kidney donors ($n = 10$ donors) biopsied to evaluate single or double allocation [20], in accordance to the Italian Clinical Guidelines published by the Italian National Transplant Centre (CNT) (http://www.-

trapianti.salute.gov.it). Due to the retrospective nature of this specimens, registration or approval by the ethics committee was waived.

Statistics

We used paired or unpaired 2-tailed *t* tests for 2-group comparisons and 1-way or 2-way ANOVA (with Tukey test for post hoc pairwise differences) for multiple independent group comparisons. Linear regression analysis was used to test the association between urinary C3a and proteinuria in FSGS patients. A 2-tailed *P* value of less than 0.05 was regarded as statistically significant. All statistical analyses were performed using GraphPad Prism (version 7 for Windows, GraphPad Software Inc.).

Study approval

Animal study protocols were approved by the Institutional Animal Care and Use Committee at Icahn School of Medicine at Mount Sinai (New York, NY).

The human studies were carried out in accordance with the principles of the Declaration of Helsinki, and all procedures were approved by the Human Subjects Committee at participating sites. All participants provided informed consent.

RESULTS

ADR-induced FSGS associates with reduced DAF expression and complement activation in BALB/c mice

We initially analyzed glomerular patterns of DAF expression in naive BALB/c mice kidneys (a strain known to be susceptible to ADR [Wang et al., 2000]) by immunofluorescence (IF). We observed strong DAF staining that colocalized with synaptopodin, indicative of podocyte expression in naive animals (Fig. 1 A). 1 wk after ADR administration, we observed markedly decreased glomerular DAF expression (Fig. 1, B and C), accompanied by glomerular C3b deposition (Fig. 1, D–F), the latter consistent with DAF's physiological function of restraining local complement activation [21].

To begin testing for functional links between DAF expression and ADR-induced kidney disease, we injected ADR into male and female WT or germline DAF−/− BALB/c mice. These experiments showed significantly more albuminuria (Fig. 1 G) with more severe histological changes (Fig. 1 H) in the DAF-deficient BALB/c mice, regardless of sex (Fig.

1 I), noting that females are more resistant to ADR-initiated glomerular injury, consistent with previous reports and with human studies [22-24].

Genetically determined DAF absence confers ADR susceptibility in B6 mice

We next investigated the relationship between DAF expression and FSGS in C57BL/6 (B6) mice, a strain that is resistant to the development of ADR-induced FSGS lesions [25]. While ADR administration did not induce proteinuria or glomerulosclerosis in WT B6 mice [25], ADR remarkably induced proteinuria and glomerulosclerosis or tubular atrophy/interstitial sclerosis in congenic B6 DAF−/− mice (Fig. 1, J–M), associated with increased glomerular C3b deposition. Because DAF has complement-independent functions, we performed additional control studies to verify that ADR-induced FSGS in DAF-deficient mice is complement dependent (Fig. 1, J–M). ADR administration to DAF−/−C3−/− mice indeed did not result in proteinuria, glomerulosclerosis, or tubular sclerosis.

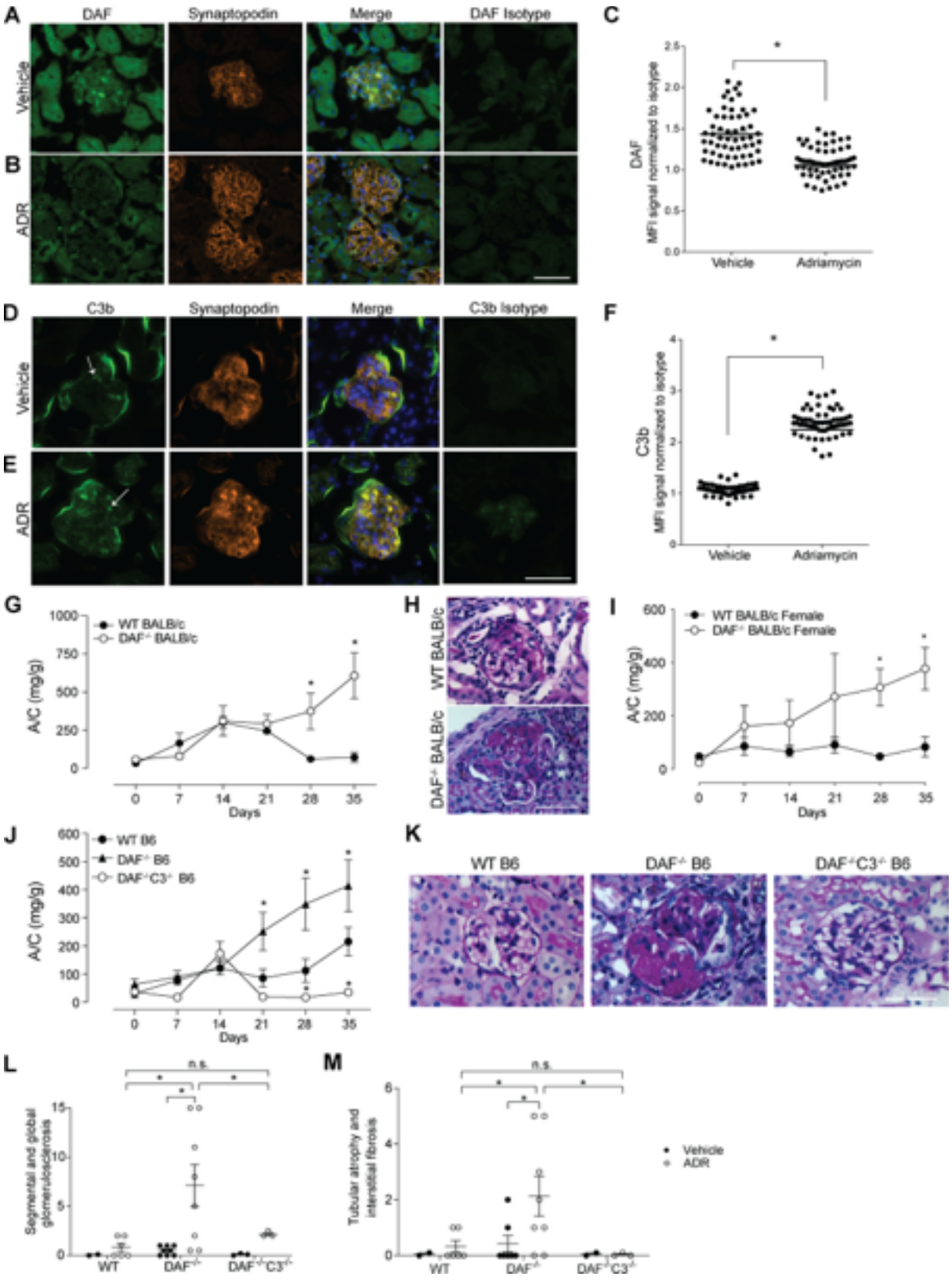
A
DAF
Synaptopodin
Merge
DAF Isotype
Vehicle
B
ADR
C
DAF
MFI signal normalized to isotype
Vehicle
Adriamycin
D
C3b
Synaptopodin
Merge
C3b Isotype
Vehicle
E
ADR
F
C3b
MFI signal normalized to isotype
Vehicle
Adriamycin
G
WT BALB/c
DAF-/- BALB/c
A/C (mg/g)
Days
H
WT BALB/c
DAF-/- BALB/c
I
WT BALB/c Female
DAF-/- BALB/c Female
A/C (mg/g)
Days
J
WT B6
DAF-/- B6
DAF-/-C3-/- B6
A/C (mg/g)
Days
K
WT B6
DAF-/- B6
DAF-/-C3-/- B6
L
n.s.
Segmental and global glomerulosclerosis
WT
DAF-/-
DAF-/-C3-/-
M
n.s.
Tubular atrophy and interstitial fibrosis
Vehicle
ADR
WT
DAF-/-
DAF-/-C3-/-

Figure 1.

Figure 1. Glomerular DAF downregulation promotes murine ADR-induced FSGS through a complement-mediated mechanism.

(A–F) Representative pictures and data quantification of glomerular (A–C) DAF and (D–F) C3b staining of male WT BALB/c mice treated with vehicle or ADR (10 mg/kg, i.v.). Background staining for C3b is present in the periphery of all glomeruli, with higher intraglomerular C3b staining (arrows) in the ADR-treated animals. DAF and C3b glomerular fluorescence intensity was quantified relative to isotype using ImageJ software. At least 30 glomeruli per mouse from two animals were included in the analysis. Each dot represents a glomerulus. (G and H) Urinary A/C at weekly intervals (G) and representative renal histological (PAS stain) lesions (H) of male WT (n = 8) or DAF−/− (n = 9) BALB/c mice sacrificed at 5 wk after ADR injection (10 mg/kg, i.v.). (I) Urinary A/C at weekly intervals of female WT (n = 5) or DAF−/− (n = 4) BALB/c mice sacrificed at 5 wk after ADR injection (10 mg/kg, i.v.). (J–M) Urinary A/C at weekly intervals (J) and representative renal histological (PAS) lesions (K) with data quantification (L and M) of male WT (n = 18), DAF−/− (n = 13), or DAF−/−C3−/− (n = 4) B6 mice sacrificed at 5 wk after ADR injection (20 mg/kg, i.v.). All experimental data were verified in at least three independent experiments. *P < 0.05 versus WT at the same time point. n.s., not significant. Scale bars: 50 μm. Error bars are SEM.

Podocyte-specific DAF-null mice are more susceptible to ADR

DAF is an intrinsic complement regulator that limits complement activation only on the cells on which it is expressed [21], raising the possibility that DAF expression specifically on podocytes locally regulates the ADR-induced, complement-dependent podocyte injury in this model. To test this, we newly generated B6 DAFfl/fl mice and crossed them to podocin-CrePOS animals (Fig. S2 A) and confirmed selective absence of DAF from podocyte surfaces (but detection on tubular cells) in these DAFfl/fl podocin-CrePOS mice (Fig. S2, B–E). DAFfl/fl podocin-CrePOS mice are healthy without growth abnormalities and do not spontaneously develop proteinuria, renal insufficiency, or other renal functional abnormalities when followed for up to 12 mo of age (data not shown). Whereas ADR injection did not induce proteinuria or glomerulosclerosis in the DAFfl/fl podocin-CreNEG control animals (Fig. 2, A and B), ADR administration to DAFfl/fl podocin-CrePOS animals resulted in albuminuria by day 21 along with histological evidence of glomerulosclerosis and tubular atrophy/interstitial sclerosis, the latter similar in severity to the lesions in germline DAF−/− mice (Fig. 2, A, C, E, and F). As an additional control,

we also generated DAFfl/fl CD11c-CrePOS mice that lack DAF on myeloid immune cells. In these animals, ADR injection did not induce proteinuria or glomerulosclerosis and tubular atrophy/interstitial sclerosis, a result that did not differ from the ADR-injected DAFfl/fl podocin-CreNEG control animals (Fig. 2, A, B, and D–F). At 35 d after ADR injection, ultrastructural analysis showed no abnormalities in vehicle-injected animals, but ADR resulted in significantly higher podocyte foot process effacement in DAFfl/fl podocin-CrePOS animals versus podocin-CreNEG control animals (Fig. 2, G and H). Together the data newly support the conclusion that podocyte-expressed DAF is protective in this model system.

To provide insight into the complement-dependent mechanisms that result in glomerular injury without DAF, we stained kidneys from DAFfl/fl podocin-CreNEG and podocin-CrePOS mice after ADR injection for complement activation products. These analyses showed increased glomerular deposition of C3b, without C1q or C4b in DAFfl/fl podocin-CrePOS compared with podocin-CreNEG control animals (Fig. 2, F–J), implicating complement activation predominantly via the alternative pathway.

Phenotypic expression of FSGS requires C3aR

Building on (1) the above data (Fig. 1; Fig. 2, A–C; Fig. S1; and Fig. S2, B–E), (2) DAF's known mechanism of restraining complement activation at the C3 convertase step, and (3) our previous reports that DAF deficiency augments C3a production [8], we postulated that, without DAF, locally produced C3a ligates podocyte-expressed C3aR to function as a crucial driver of the podocyte injury in this model. After documenting that podocytes express C3aR and that C3aR expression is increased 2 wk after ADR injection (Data not shown), we administered ADR to groups of germline DAF−/−C3aR−/−

mice and to WT and DAF−/− control animals (Fig. 2, I and J). These experiments showed that germline C3aR deficiency fully prevented the ADR-induced FSGS observed in DAF-deficient mice. We observed similar protection against FSGS development in ADR-administered BALB/c mice treated with the selective C3aR antagonist (C3aR-A) SB290157 (1 mg/kg/d s.c. for 28 d by injection pumps; Fig. 2, K and L). C3aR-A administration to ADR-treated BALB/c mice also showed significantly less albuminuria than untreated control animals after ADR injection (albumin/creatinine [A/C], 253 ± 59 versus 752 ± 97 mg/g; $P < 0.05$). When we administered ADR to B6 DAFfl/fl podocin-CrePOS with or without C3aR-A, we also observed a significant decrease in the clinical and histological manifestations of kidney disease (Fig. 2, M and N).

Figure S2.

Figure S2.

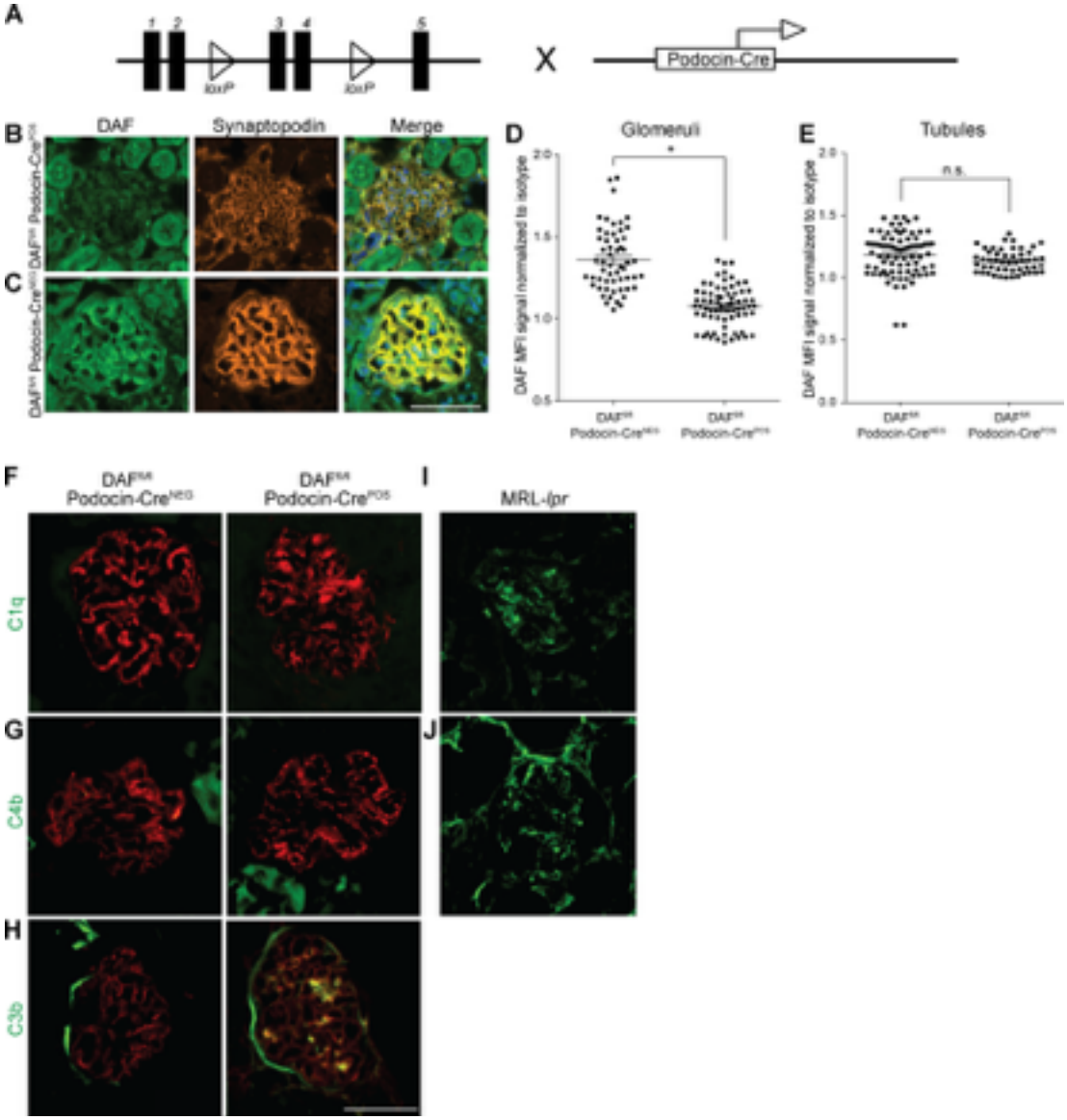

Podocyte-specific DAF-KO mice show increased glomerular C3b deposition in the absence of C1q or C4b deposits in

response to ADR. (A) Schematic demonstrating the breeding of the DAFfl/fl mice with the podocin-Cre mice to generate DAFfl/fl podocin-CrePOS animals. (B–E) Representative pictures of renal staining of DAF expression in the glomeruli and tubules (B and C) and data quantification (D and E) from 8-wk-old male DAFfl/fl podocin-CrePOS and podocin-CreNEG mice. DAF glomerular and tubular fluorescence intensity were quantified as in Fig. 1. (F–J) Representative glomerular C1q (F), C4 (G), and C3b (H) staining in B6 DAFfl/fl podocin-CreNEG and podocin-CrePOS mice at 2 wk after ADR injection. Synaptopodin is stained in red. As positive controls for C1q and C4b, we used MRL-lpr lupus-prone mice at 4 mo of age (I and J). All experimental data were verified in at least three independent experiments. n.s., not significant. Scale bars: 50 μm. *P < 0.05. Error bars are SEM.

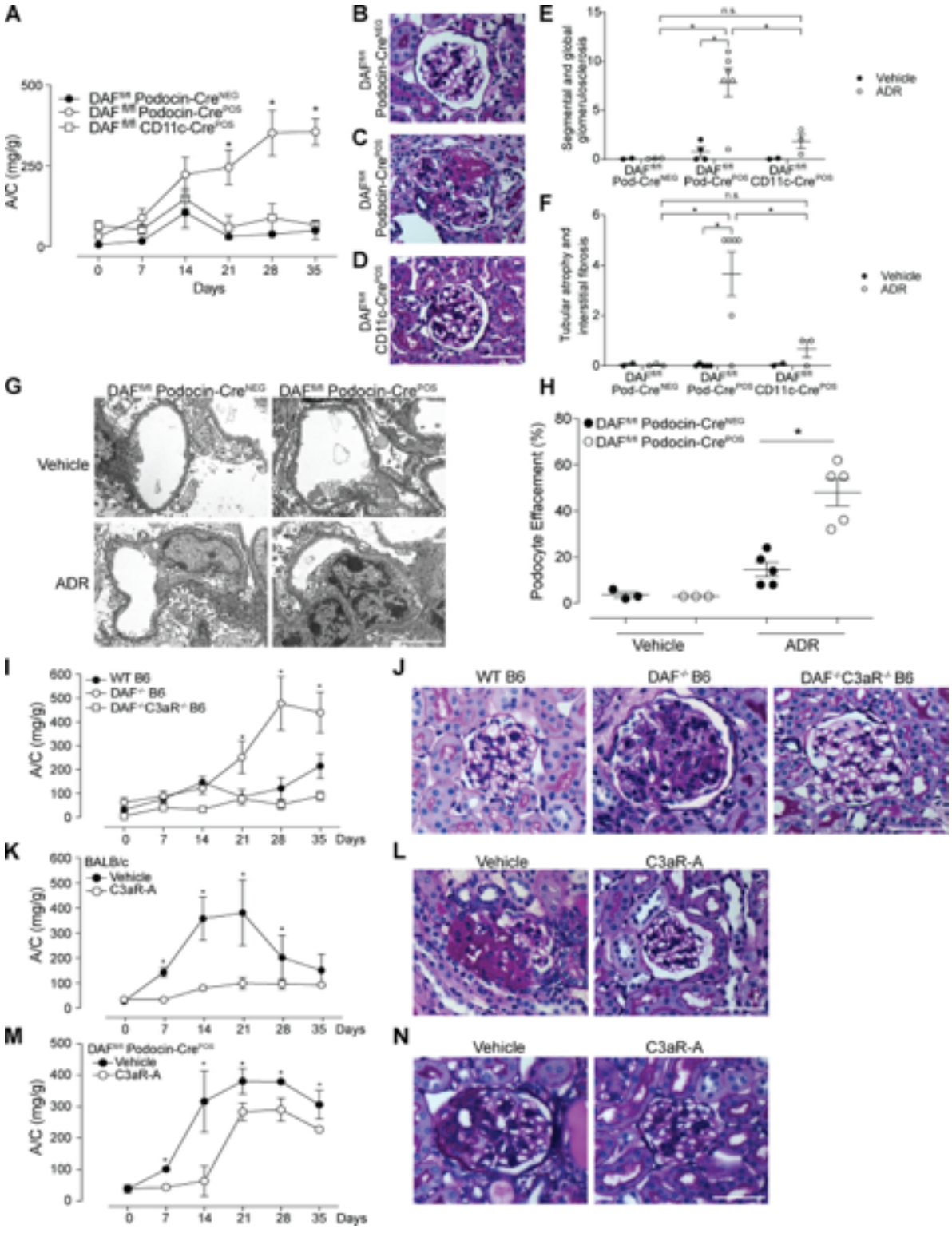
A
B
C
D
E
F
G
H
I
J
K
L
M
N
A/C (mg/g)
Days
DAF f/f Podocin-Cre NEG
DAF f/f Podocin-Cre POS
DAF f/f CD11c-Cre POS
Segmental and global glomerulosclerosis
Tubular atrophy and interstitial fibrosis
Vehicle
ADR
Podocyte Effacement (%)
WT B6
DAF-/- B6
DAF-/-C3aR-/- B6
BALB/c
C3aR-A

Figure 2

Figure 2. Podocyte-specific removal of DAF from podocytes increases susceptibility to ADR-induced injury through C3a/C3aR signaling. (A–F) Urinary A/C at weekly intervals (A) and representative renal histological (PAS) lesions (B–D) with data quantification (E and F) of male DAFfl/fl podocin-CreNEG (n = 10), DAFfl/fl podocin-CrePOS (n = 19), and DAFfl/fl CD11c-CrePOS (n = 5) mice injected with ADR (20 mg/kg, i.v.) and sacrificed after 5 wk. (G and H) Representative electron micrographs (G) and quantification (H) of podocyte effacement in 8-wk-old DAFfl/fl podocin-CrePOS or DAFfl/fl podocin-CreNEG mice at 5 wk after treatment with saline or ADR (20 mg/kg, i.v.). (I and J) Urinary A/C at weekly intervals (I) and representative renal histological (PAS) lesions (J) of WT (n = 16), DAF−/− (n = 13), and DAF−/−C3aR−/− (n = 4) male B6 mice injected with ADR (20 mg/kg, i.v.). (K and L) Urinary A/C at weekly intervals (K) and representative renal histological (PAS) lesions (L) of male BALB/c mice given ADR (10 mg/kg, i.v.) and treated with C3aR-A (1 mg/kg/d, s.c.; n = 5) or saline (n = 5). (M and N) Urinary A/C at weekly intervals (M) and representative renal histological (PAS) lesions (N) of male B6 DAFfl/fl podocin-CrePOS mice given ADR (20 mg/kg, i.v.) and treated with C3aR-A (1 mg/kg/d, s.c.; n = 5) or saline (n = 5). *P < 0.05 versus podocin-CreNEG, WT, or C3aR-A. All experimental data were verified in at least three independent experiments. n.s., not significant. Scale bars: 50 μm. Error bars are SEM.

ADR promotes phospholipase D–mediated cleavage of DAF from podocyte surfaces

Our data thus far indicate that ADR-induced DAF downregulation on podocytes contributes to the development of glomerulosclerosis. To discern the molecular mechanisms underlying this ADR-induced decrease in DAF expression, we quantified Daf mRNA (qPCR) in kidneys from BALB/c mice treated with vehicle or ADR. These experiments surprisingly showed significantly more Daf gene expression after ADR injection (3.9 ± 2.1-fold versus 1.1 ± 0.4-fold, respectively; $P < 0.05$; $n = 3$ animals per group), despite the above observed decrease in glomerular DAF by IF staining. In vitro cultures of immortalized human podocytes (hiPod) with or without ADR similarly showed that ADR augmented Daf gene expression (2.3 ± 0.1-fold versus 1.0 ± 0.1-fold, respectively; $P < 0.01$; $n = 3$ experiments per group), but they showed decreased DAF on cell surfaces (Fig. 3, A and B).

DAF is a GPI-anchored membrane protein that can be cleaved by phospholipases, including, among others, phospholipase D (PLAD), raising the possibility that ADR-induced DAF surface protein downregulation is mediated by PLAD-dependent GPI cleavage. We observed increased Gpld1 gene expression in the kidneys from BALB/c mice 1 wk after ADR treatment compared with saline injection (4.4 ± 1.0-fold versus 1.0 ± 0.2-fold, respectively; $P < 0.05$) and in hiPod exposed to ADR compared with vehicle-treated cells for 24 h (2.0 ± 0.6-fold versus 1.0 ± 0.1-fold, respectively; $P < 0.05$). Immunoblots of hiPod showed a significant increase in PLAD protein following ADR expo-

sure (Fig. 3, C and D). To test for a causal link between PLAD expression and DAF cleavage, we exposed podocytes to ADR in the presence or absence of a selective PLAD inhibitor (PLADi). Consistent with the hypothesis that ADR promotes DAF cleavage by increasing PLAD expression, the PLADi preserved membrane expression of DAF in podocytes exposed to ADR (Fig. 3, A and B). Addition of the PLADi also reduced soluble DAF in the supernatants of podocytes exposed to ADR, supporting the hypothesis that PLAD reduces DAF expression through GPI cleavage (Fig. 3, E and F). When we tested the urine of WT BALB/c mice 2 wk after injection with ADR or vehicle control, we found cleaved DAF in ADR-treated animals (but not in control animals), further supporting the conclusion that ADR induces glomerular DAF cleavage in vivo (Fig. 3 G).

Figure 3.

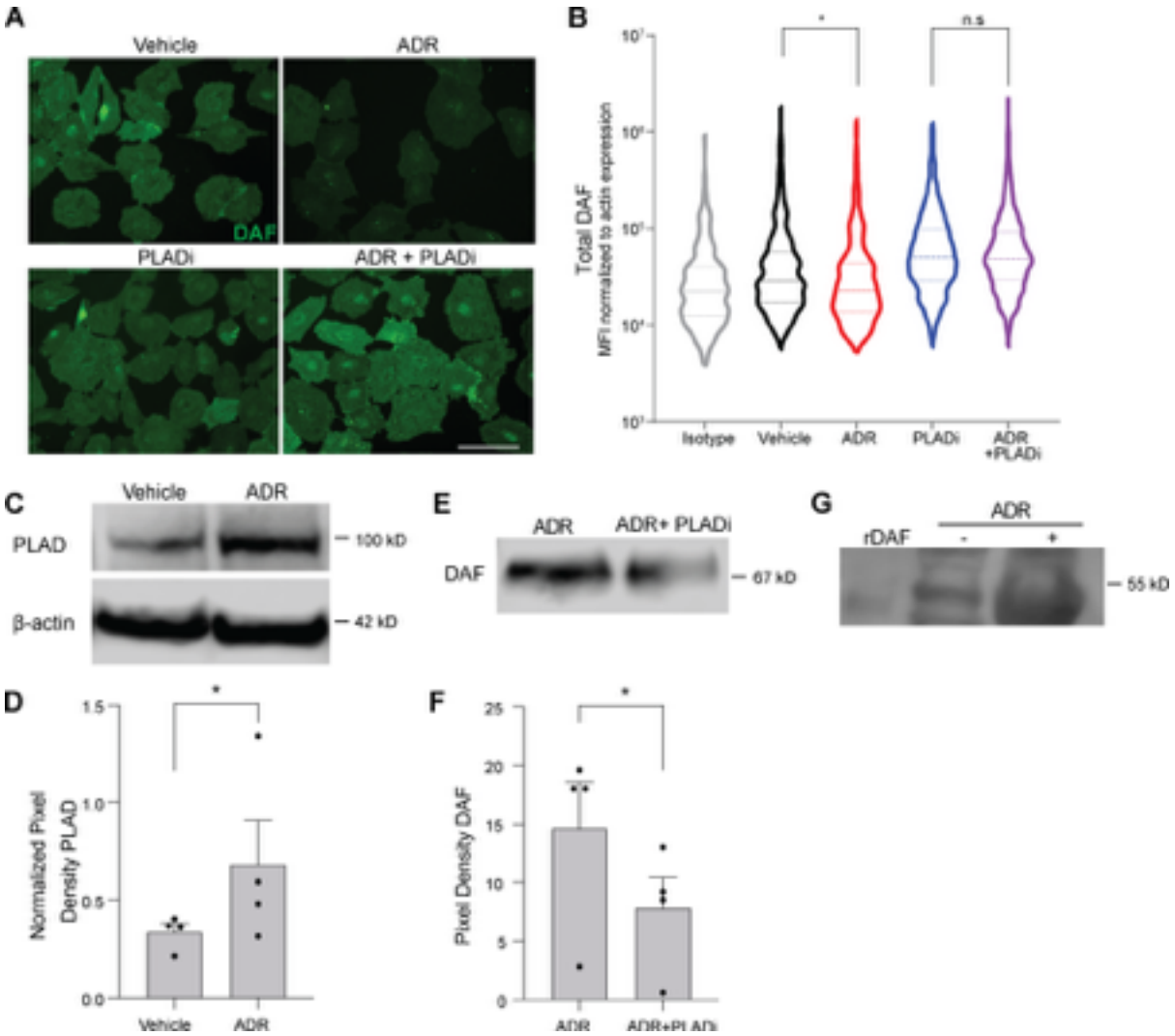

Figure 3.

Figure 3. ADR induces PLAD-dependent cleavage of DAF. (A and B) Representative images (A) and distribution of DAF expression (B) quantified in hiPod exposed to vehicle, ADR (0.3 μg/ml), PLADi (1 μM), or ADR + PLADi (0.3 μg/ml in 1 μM) for 24 h. DAF IF signal was normalized to actin expression pixel by pixel, and the MFI for each cell was computed. Results are representative of two independent experiments with similar results. (C and D) Representative blots (C) and densitometric analysis (D) of PLAD expression in hiPod cell lysates previously exposed to vehicle or ADR for 24 h. (E and F) Representative blots (E) and densitometric analysis (F) of DAF in the supernatants of hiPod exposed to ADR for 24 h with or without PLADi (WB). (G) Representative blot of DAF in the urine from BALB/c male mice at 2 wk after treatment with vehicle or ADR compared with recombinant mouse DAF (rDAF). In each group, we

pooled and concentrated urine samples from eight mice (see Materials and methods). All experimental data were verified in at least three independent experiments. *P < 0.05; n.s., not significant. Scale bars: 50 μm. Error bars are SEM.

DAF-deficient mice are more susceptible to STZ-induced diabetic kidney disease

To test the hypothesis that DAF cleavage and associated complement activation modulate clinical and histological expression of another form of glomerulosclerosis, we studied mice with STZ-induced type 1 diabetic kidney disease, which is manifested pathologically by increased mesangial expansion and sclerosed glomeruli [26]. In this model, STZ associated with glomerular deposition of C3b (Fig. 4, A and B). Whereas WT BALB/c mice 20 wk after STZ show modest albuminuria and glomerular lesions (Fig. 4, C and D), STZ-treated DAF−/− mice show significantly higher urinary albumin (Fig. 4 C) and more severe glomerular changes (Fig. 4 D), despite similar levels of hyperglycemia between groups (Fig. 4 E). STZ-treated B6 DAFfl/fl podocin-CrePOS mice lacking DAF on podocytes had higher levels of C3b deposition in the glomeruli than control animals (Fig. 4, F and G), which was associated with more severe diabetic kidney disease (Fig. 4, H and I) despite similar glycemic levels (Fig. 4 J). Together the findings newly implicate DAF deficiency specifically on podocytes and resultant complement activation as contributing to the pathogenesis of this form of glomerulosclerosis as well as to FSGS.

Figure 4.

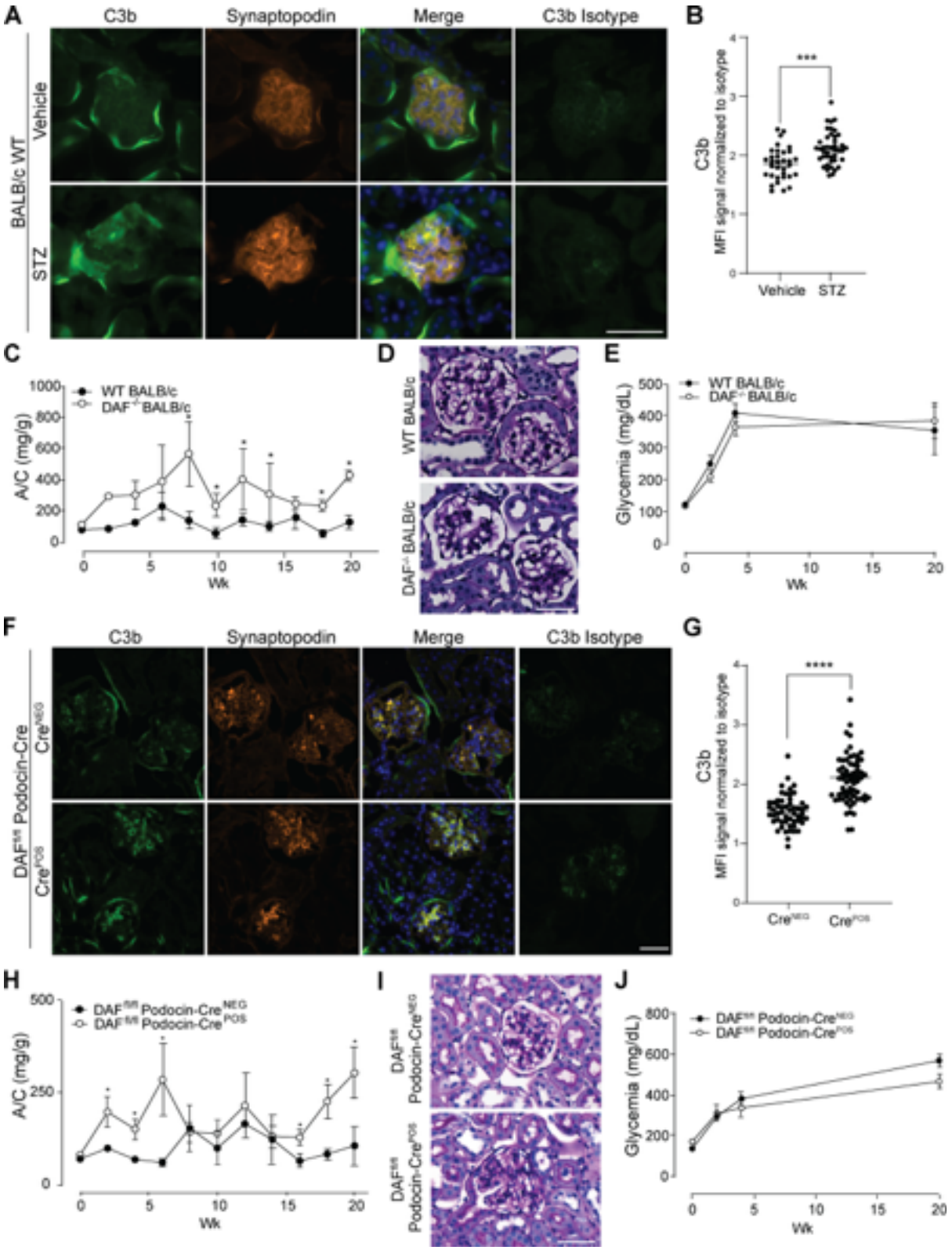
A
C3b
Synaptopodin
Merge
C3b Isotype
BALB/c WT
Vehicle
STZ
B
C3b
MFI signal normalized to isotype
***
Vehicle
STZ
C
WT BALB/c
DAF-/- BALB/c
A/C (mg/g)
Wk
D
WT BALB/c
DAF-/- BALB/c
E
WT BALB/c
DAF-/- BALB/c
Glycemia (mg/dL)
Wk
F
C3b
Synaptopodin
Merge
C3b Isotype
DAFfl/fl Podocin-Cre
CreNEG
CrePOS
G
C3b
MFI signal normalized to isotype
****
CreNEG
CrePOS
H
DAFfl/fl Podocin-CreNEG
DAFfl/fl Podocin-CrePOS
A/C (mg/g)
Wk
I
DAFfl/fl Podocin-CreNEG
DAFfl/fl Podocin-CrePOS
J
DAFfl/fl Podocin-CreNEG
DAFfl/fl Podocin-CrePOS
Glycemia (mg/dL)
Wk

Figure 4. Glomerular DAF downregulation promotes murine STZ-induced diabetic kidney disease.

(A and B) Representative pictures (A) and data quantification (B) of glomerular C3b in BALB/c WT mice at 5 wk after vehicle or STZ injection. ***P < 0.001. (C and D) Urinary A/C at weekly intervals (C) and representative renal histological (PAS) lesions (D) of male WT (n = 8) or DAF−/− (n = 5) BALB/c mice sacrificed at 5 wk after STZ injection (50 mg/kg, i.p., for five consecutive days). *P < 0.05 versus WT at the same time point. (E) Glycemic levels of mice injected with STZ shown in A–D. (F and G) Representative pictures (F) and data quantification (G) of glomerular C3b in DAFfl/fl podocin-CreNEG/POS B6 mice at 5 wk after STZ injection. ****P < 0.001. (H and I) Urinary A/C at weekly intervals (H) and representative renal histological (PAS) lesions (I) of male DAFfl/fl podocin-CreNEG (n = 9) or podocin-CrePOS (n = 8) B6 mice sacrificed at 20 wk after STZ injection (50 mg/kg, i.p., for five consecutive days). *P < 0.05 versus DAFfl/fl podocin-CreNEG at the same time point. (J) Glycemic levels of mice injected with STZ shown in H and I. Only mice that reached glycemia >300 mg/dl at 2 wk after STZ injection were included in this set of experiments. All experimental data were verified in at least three independent experiments. Scale bars: 50 μm. Error bars are SEM.

DAF and complement in human FSGS and diabetic kidney disease

To test whether the above murine findings potentially apply to humans with FSGS and diabetic kidney disease, we examined data from one large published RNA-sequencing study using Nephroseq (http://www.nephroseq.org/). The study compared expression levels of RNA extracted from microdissected glomerular samples from patients with FSGS (n = 17), diabetic nephropathy (n = 12), and control individuals (kidney living donors; n = 35). Our analyses showed significantly increased expression of mRNA for C3, C3aR, and C5aR in samples from patients with FSGS or diabetic kidney disease compared with control individuals (Fig. 5, A–C), providing associative evidence that the complement system is implicated in the pathogenesis of human diseases. In the same FSGS and diabetic kidney disease patients, we also observed increased DAF mRNA expression in the diseased kidneys versus control individuals (Fig. 5 D). When we stained kidney biopsies from 18 patients with FSGS, we observed increased C3d deposition compared with control individuals (Fig. 5, E and F; Table 1). Consistent with murine data (Fig. 1, A–C), DAF staining of glomeruli with FSGS (n = 18) showed weaker expression than control kidneys (n = 10; Fig. 5, G and H). As one approach to test whether the lower DAF expression results in complement activation in the kidney, we quantified urinary C3a and proteinuria in urine samples from 27 patients with FSGS and in 10 healthy control individuals (Fig. 5, I–L; Table 2). These analyses showed a significant correlation between urinary C3a and proteinuria at the time of diagnosis in the FSGS cohort (Fig. 5 I), while no C3a was detected in the urine of healthy control individuals. We observed that the elevations in proteinuria and urinary C3a were significantly reduced after therapy (Fig. 5, J and K), and their changes correlated with one another

(Fig. 5 L). Together with previous observations by others [27], our data support the concept that complement components are present in the urinary space of subjects with proteinuria and are activated by DAF downregulation, leading to the formation of C3a and C5a.

We also tested for cleaved DAF in the urine of patients with FSGS and healthy control individuals by immunoblotting. These assays showed that soluble/cleaved DAF was detectable in the urine of patients with FSGS but not in healthy control individuals, further supporting the concept that DAF reduction observed in patients with FSGS is due to its cleavage (Fig. 5 M).

Figure 5.

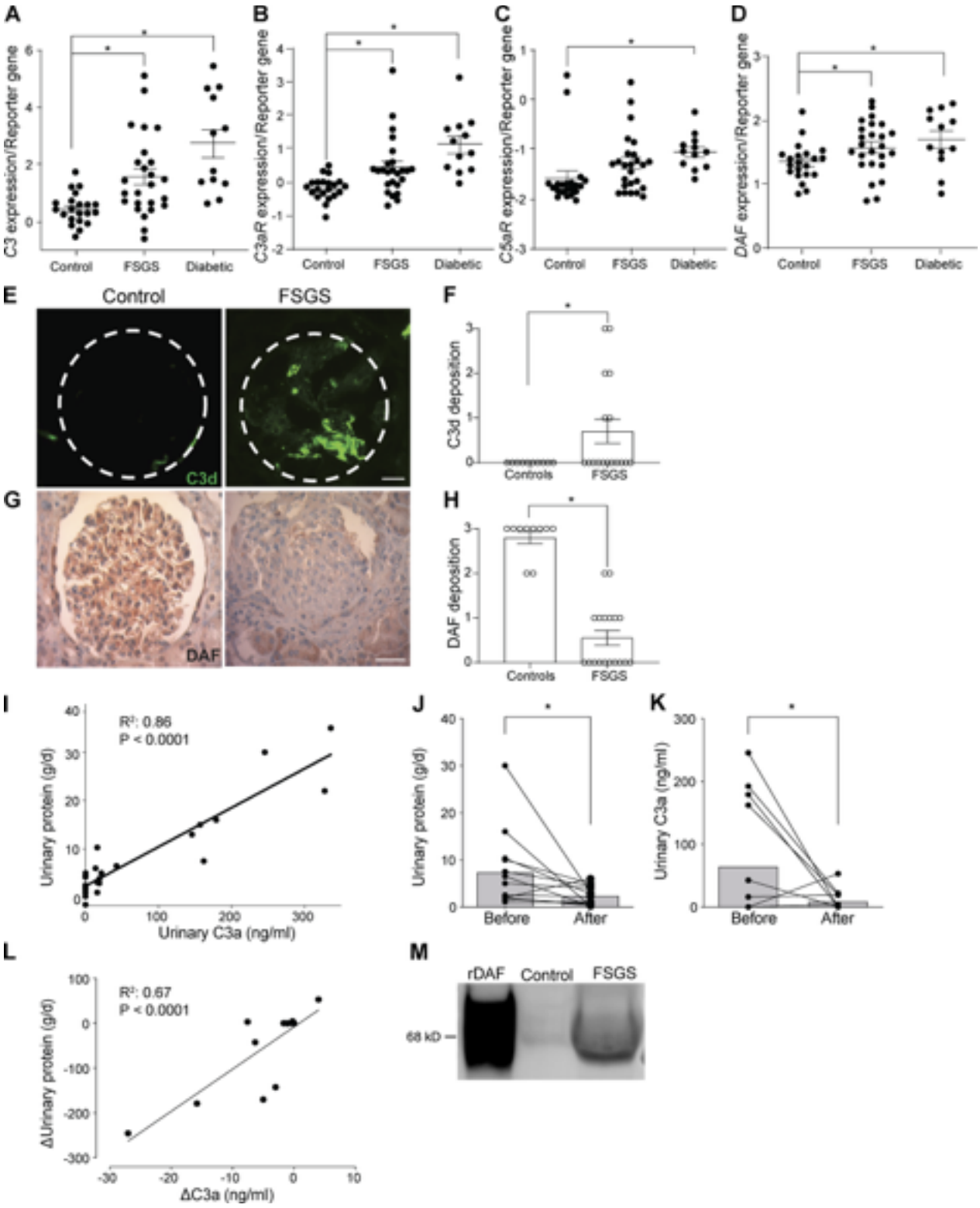
A
C3 expression/Reporter gene
Control
FSGS
Diabetic
B
C3aR expression/Reporter gene
C
C5aR expression/Reporter gene
D
DAF expression/Reporter gene
E
Control
FSGS
C3d
F
C3d deposition
Controls
FSGS
G
DAF
H
DAF deposition
I
R²: 0.86
P < 0.0001
Urinary protein (g/d)
Urinary C3a (ng/ml)
J
Before
After
K
Urinary C3a (ng/ml)
L
R²: 0.67
P < 0.0001
ΔUrinary protein (g/d)
ΔC3a (ng/ml)
M
rDAF
Control
FSGS
68 kD

Figure 5. FSGS in humans is associated with DAF down-regulation and complement activation. (A–D) C3 (A), C3aR (B), C5aR (C), and DAF mRNA (D) expression in glomeruli of human biopsy specimens with pathological diagnosis of FSGS or diabetic kidney disease compared with normal kidneys. Data are from previously published microarray studies by Ju et al. (2013) and were subjected to further analysis using Nephroseq. (E–H) Representative renal staining and data quantification for C3d (IF; E and F) and DAF (immunohistochemistry; G and H) in patients with FSGS (n = 18) and in kidneys from healthy renal donors (n = 10). (I) Correlation between protein and C3a in urine samples from 27 patients with FSGS taken at the time of kidney biopsy (before therapy). (J and K) Differences in proteinuria (J) and urinary C3a (K) measured before versus 3–6 mo after steroid therapy in a subset of 13 patients with FSGS. (L) Correlation between the change in proteinuria and change in urinary C3a before and after therapy for each of the same 13 patients. (M) Representative blot of DAF in the urine from healthy control individuals and patients with FSGS compared with recombinant human DAF (rDAF). In each group, we pooled and concentrated urine samples from five and five subjects, respectively (see Materials and methods). *P ≤ 0.05. Scale bars: 25 µm. Error bars are SEM.

C3a/C3aR signaling promotes actin cytoskeleton rearrangement in human podocytes

Absence of surface DAF lifts restraint on local complement activation, resulting in production of C3a [8]. As our above data (Fig. 2, I–N) showed that C3aR signaling on podocytes drives ADR-induced FSGS, we next tested molecular links between C3a/C3aR and podocyte injury. After verifying that cultured hiPod express C3aR (data not shown), we exposed them to recombinant C3a for 24 h and used IF to quantify actin cytoskeleton expression and distribution because they are functionally linked to podocyte structure and permselectivity [28]. C3a induced rearrangement of actin cytoskeleton (Fig. 6, A and B), an effect that was prevented by the selective C3aR antagonist SB290157 but not vehicle control (Fig. 6, A and B), implicating C3aR as the mediator of C3a effects. To test for the effect of C3a on podocyte viability, we stained the cells for caspase-3 (apoptotic marker), and we showed that C3a–C3aR interaction promotes cell apoptosis as well (Fig. 6 C). We similarly observed C3a/C3aR-induced cytoskeleton rearrangement of human podocytes derived from amniotic fluid kidney progenitor cells [19, 29] (Fig. 6, D and E).

Data from studies performed in both human and mouse podocytes show that podocyte damage (including damage caused by C3a/C3aR1 signaling) increases expression of Snail that, in turn, decreases nephrin expression and disrupts the slit diaphragm [30]. In accordance with these observations by others, addition of C3a increased podocyte Snail and TGF-β protein expression in cultured human podocytes, and the effects were prevented by addition of a C3aR antagonist (Fig. 6, F and G).

To provide additional mechanistic insight, we used a protein array to measure changes in 105 cytokines and mediators of kidney injury from supernatants of hiPod exposed to vehicle, C3a, or C3a plus C3aR-A for 24 h. These analyses showed that C3a selectively increased 16 of the molecules in the array (Fig. 6 H). We used the Genome-scale Integrated Analysis of Gene Networks in Tissues (GIANT, now HumanBase) Bayesian integration (Wong et al., 2018) to capture the most relevant podocyte-specific functional interactions between C3aR and nephrin, a major component of the slit diaphragm. Each interaction (or functional relationship) in the networks generated represents a body of data, probabilistically weighted and integrated, focused on a particular biological question/tissue. Of the 16 molecules selectively upregulated by C3a (but not by C3a + C3aR-A) the GIANT analyses indicated that IL-1β provided the strongest predicted functional connection between C3aR and nephrin selectively in podocytes (Fig. 6 I).

Figure 6.

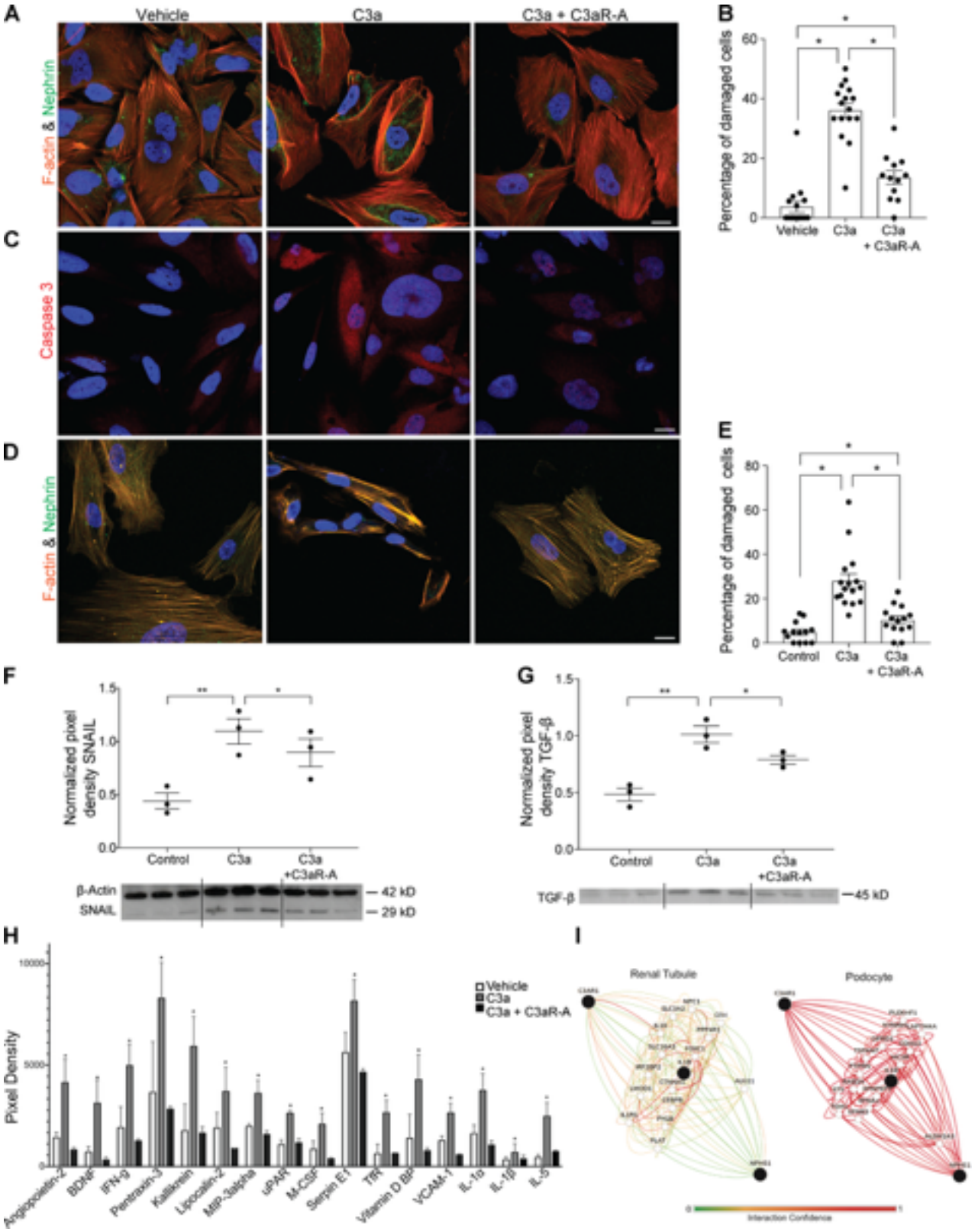
A
Vehicle
C3a
C3a + C3aR-A
F-actin & Nephrin
B
Percentage of damaged cells
Vehicle
C3a
C3a + C3aR-A
C
Caspase 3
D
F-actin & Nephrin
E
Percentage of damaged cells
Control
C3a
C3a + C3aR-A
F
Normalized pixel density SNAIL
Control
C3a
C3a +C3aR-A
β-Actin
SNAIL
42 kD
29 kD
G
Normalized pixel density TGF-β
Control
C3a
C3a +C3aR-A
TGF-β
45 kD
H
Pixel Density
Vehicle
C3a
C3a + C3aR-A
Angiopoietin-2
BDNF
IFN-g
Pentraxin-3
Kallikrein
Lipocalin-2
MIP-3alpha
uPAR
M-CSF
Serpin E1
TIR
Vitamin D BP
VCAM-1
IL-1α
IL-1β
IL-5
I
Renal Tubule
Podocyte
Interaction Confidence

Figure 6. C3a–C3aR interaction disrupts actin cytoskeleton in human cultured podocytes. (A and B) Representative images (A) and quantification (B) of cell injury of hiPod exposed to vehicle, C3a (50 nM), or C3a + C3aR-A (50 nM) for 24 h and stained for F-actin and nephrin. (C) Representative images of caspase-3 staining of the same cells pictured above. (D and E) Representative images (D) and quantification (E) of cell injury of amniotic fluid–derived human podocytes exposed to vehicle, C3a (50 nM), or C3a + C3aR-A (50 nM) for 24 h and stained for F-actin and nephrin. *P < 0.05. (F and G) Representative blots and densitometric analysis of Snail (F) and TGF-β (G) expression in hiPod treated with vehicle, C3a, or C3a + C3aR-A for 24 h. Snail was measured in cell lysates; TGF-β was measured in cell supernatants. *P < 0.05; **P < 0.01. (H) Differentially expressed proteins in the supernatants of hiPod exposed for 24 h to vehicle, C3a (50 nM), or C3a + C3aR-A (50 nM; Proteome Profiler Human XL Cytokine Array). The cytokines represented here are the only ones among the 105 analyzed (see Materials and methods) whose expression levels significantly differed in C3a-treated podocytes versus both vehicle- and C3a + C3aR antagonist–treated cells. *P < 0.05 versus vehicle and C3a + C3aR antagonist. (I) Functional network showing the relationship between C3aR, IL-1β, and nephrin in renal tubular cells and in podocytes (https://hb.flatironinstitute.org/gene/; query genes C3aR, IL1B, and NPHS1; tissue, renal tubules or podocytes; maximum number of genes, 15). All experimental data were verified in at least two independent experiments. Scale bars: 20 μm. Error bars are SEM.

C3a/C3aR signaling is linked to podocyte injury and FSGS through IL-1β

IL-1β is a proinflammatory cytokine produced by monocytes, lymphocytes, and other cells, including podocytes [31, 32], and it is detected in glomeruli of subjects with proteinuric nephropathies, including FSGS. IL-1β is produced as a precursor (pro–IL-1β) that must be cleaved by the multiprotein inflammasome complex in order to be activated and secreted. Given that C3a/C3aR ligations transduce signals that promote IL-1β release in other cell types, including monocytes [33], we hypothesized that C3a/C3aR signaling promotes podocyte production and release of IL-1β, which in turn binds to IL-1β receptor (IL-1R1) on the same cells (paracrine and autocrine) to promote nephrin reduction and cytoskeleton rearrangement [34]. Consistent with our hypothesis, when we cultured hiPod with C3a, we observed a significant increase in IL1B transcripts (Fig. 7 A). When podocytes were cultured with LPS with or without C3a, we found that C3a significantly augmented IL-1β secretion (Fig. 7 B), the latter indicative of increased inflammasome activation [33].

To test the hypothesis that C3a-induced IL-1β production is responsible for podocyte injury, we exposed hiPod to C3a, C3a + anti–IL-1β–neutralizing antibody, or isotype IgG alone (Fig. 7 C). These experiments showed that C3a reduced nephrin expression and that the effect was abolished when C3a was administered with anti–IL-1β–neutralizing antibody but not isotype control, together supporting the conclusion that C3a-induced reduction in nephrin requires IL-1β/IL-1R1 signaling as an intermediary step.

On the basis of evidence that IL-1β induces actin cytoskeleton rearrangement through IL-1R1 signaling in podocytes, we tested whether blockade of IL-1β prevents C3a-induced effects on the cytoskeleton. C3a promoted rearrangement of the podocyte cytoskeleton, and this effect was fully prevented when cells were exposed to C3a in conjunction with anti–IL-1β–neutralizing antibody (Fig. 7, D and E).

Figure 7.

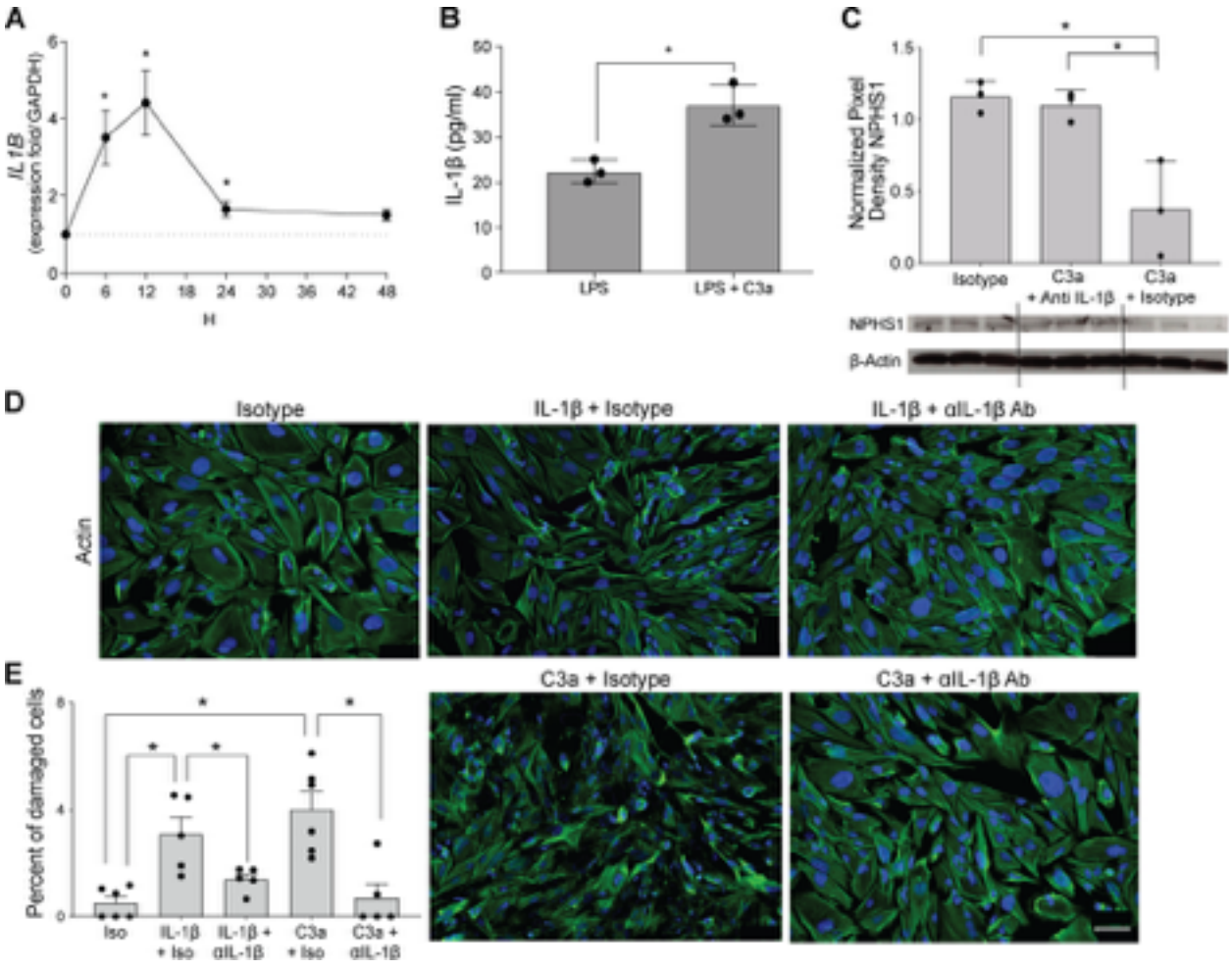

Figure 7. IL-1β mediates complement-induced podocyte injury in vitro. (A) IL1B gene expression in hiPod at serial time points after C3a stimulation (50 nM). (B) IL-1β levels in the supernatants of hiPod at 24 h after LPS (5 ng/ml) with or without C3a stimulation. (C) Nephrin expression in hiPod at 24 h after stimulation with isotype, C3a + anti–IL-1β–neutralizing antibody, and C3a + isotype (WB). *P < 0.05 versus 0 h. (D and E) Representative images (D) and quantification (E) of cell injury of hiPod exposed to isotype control, IL-1β (50 ng/ml) + isotype control, or IL-1β (50 ng/ml) + anti–IL-1β–neutralizing antibody (0.5 μg/ml; upper row). In the bottom row, the same cells were exposed to C3a + isotype control or C3a + anti–IL-1β–neutralizing antibody for 1 h. All experimental data were verified in at least two independent experiments. *P < 0.05. Scale bars: 100 μm. Error bars are SEM.

Finally, to test how the in vitro mechanisms implicating pathogenic links among C3aR, IL-1β, and podocyte dysfunction apply to the development of ADR-induced FSGS, we treated ADR-injected BALB/c mice with anti–IL-1β–neutralizing antibody or isotype control, beginning on the day of ADR injection. These experiments showed significantly lower albuminuria levels and reduced histological evidence of disease in mice treated with the neutralizing antibody (Fig. 8, A and B), despite similar amounts of C3b deposited in the glomeruli (Fig. 8, C and D). To formally test whether these protective effects are due to IL-1R signaling, we administered ADR to DAFfl/fl podocin-CrePOS and Cre-NEG littermate control animals and treated them with anakinra or vehicle control starting from the day of ADR administration. These experiments showed that IL-1R blockade with anakinra also prevented the onset of albuminuria and glomerular lesions (Fig. 8, E and F). Together with the previous experiments, the data indicate that DAF-regulated C3a/C3aR ligations on podocytes cause ADR-induced glomerular injury via an IL-1β–dependent mechanism. Data from Nephroseq analyses of glomeruli of patients with FSGS or healthy control individuals showed increased levels of IL1B and IL1R1 mRNA levels in individuals with FSGS, supporting the conclusion that similar mechanisms apply to humans (Fig. 8, G and H).

Figure 8.

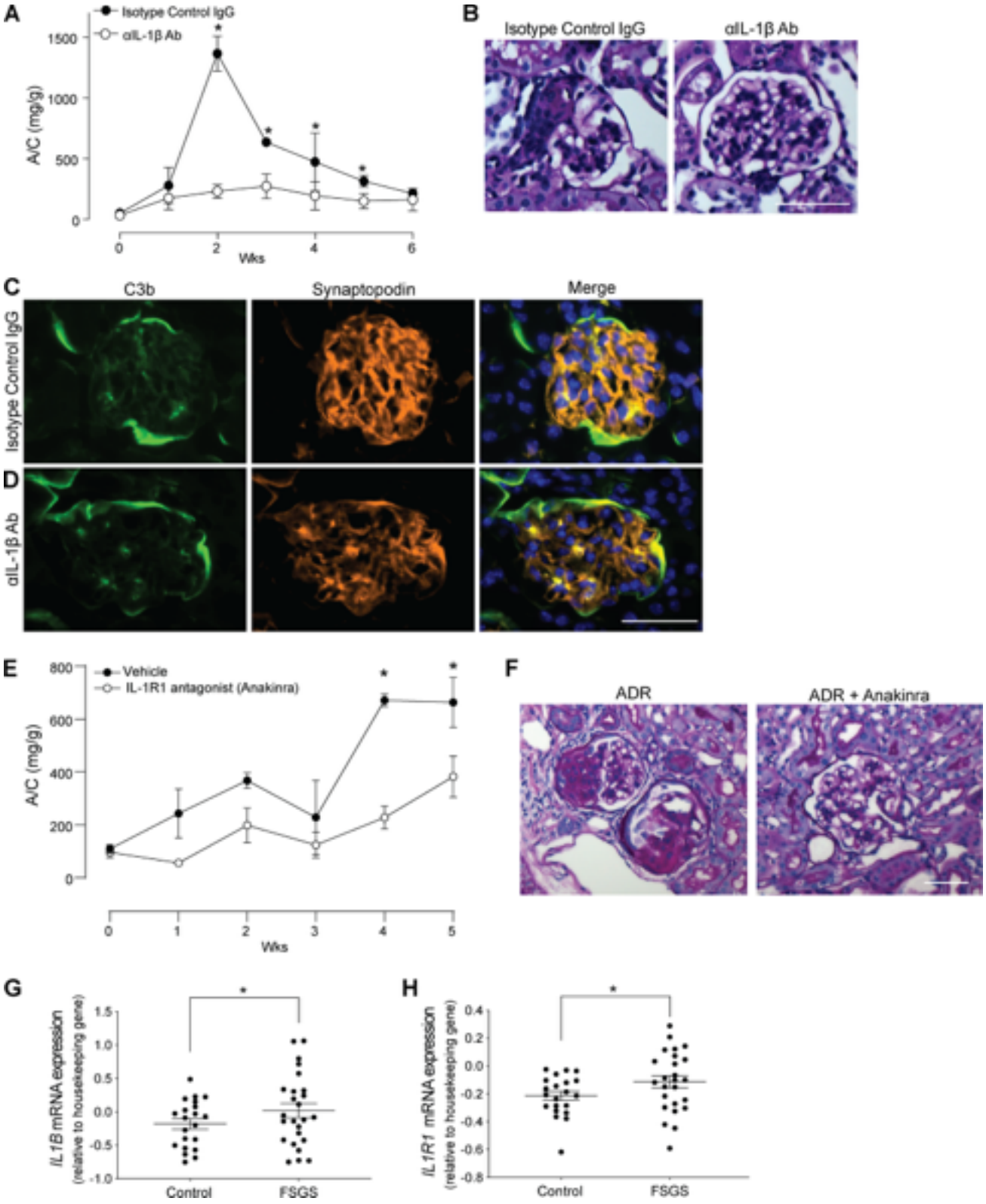
A
Isotype Control IgG
αIL-1β Ab
A/C (mg/g)
1500
1000
500
0
0
2
4
6
Wks
B
Isotype Control IgG
αIL-1β Ab
C
C3b
Synaptopodin
Merge
Isotype Control IgG
D
αIL-1β Ab
E
Vehicle
IL-1R1 antagonist (Anakinra)
A/C (mg/g)
800
600
400
200
0
0
1
2
3
4
5
Wks
F
ADR
ADR + Anakinra
G
IL1B mRNA expression
(relative to housekeeping gene)
1.5
1.0
0.5
0.0
-0.5
-1.0
Control
FSGS
H
IL1R1 mRNA expression
(relative to housekeeping gene)
0.4
0.2
0.0
-0.2
-0.4
-0.6
-0.8
Control
FSGS

Figure 8. L-1β mediates complement-induced podocyte injury in vivo. (A and B) Urinary A/C (A) and representative renal histological changes (B) in BALB/c mice injected with 10 mg/kg of ADR (i.v.) and rat anti-mouse IL-1β–neutralizing mAb (50 μg/mice twice per week, i.p.; n = 4) or isotype control (n = 4). Scale bars: 50 μm. *P < 0.05 versus anti–IL-1β–neutralizing antibody at the same time point. (C and D) Representative images of C3b deposition in the glomeruli of mice treated with (C) anti–IL-1β–neutralizing antibody or (D) isotype control. (E and F) Urinary A/C (E) and representative renal histological changes (F) in B6 DAFfl/fl podocin-CrePOS male mice injected with 10 mg/kg of ADR (i.v.) and anakinra (25 mg/kg/d through s.c. pumps; n = 4) or vehicle control (n = 3). Scale bars: 50 μm. *P < 0.05 versus anakinra at the same time point. (G and H) IL1B (G) and IL1R1 mRNA expression (H) in glomeruli of human biopsy specimens with pathological diagnosis of FSGS compared with normal kidneys. Data are from previously published microarray studies by Ju et al. (2013) and were subjected to further analysis using Nephroseq. *P < 0.05. All experimental data were verified in at least two independent experiments. Error bars are SEM.

DISCUSSION

Individuals with FSGS have often C3d deposits in the glomeruli and their presence associates with worse clinical outcomes. Our present results identify DAF cleavage on podocyte membranes as the central mechanism for complement activation in FSGS pathogenesis. Importantly, data from $DAF^{-/-}C3^{-/-}$ mice document that, in the absence of C3, mice are protected from ADR-induced FSGS, indicating that complement is required for glomerulosclerosis formation.

Deposition of C3b, but not C1q nor C4b in the glomeruli of mice with FSGS suggests that complement activation occurs mainly through the alternative pathway. This finding is consistent with previously reported data by Lenderink et al. [35] showing that mice lacking factor B (fB), a regulator of alternative complement pathway activation, develop lower proteinuria than WT controls upon ADR injection. Similarly, factor D (fD)-deficient mice show lower proteinuria and less glomerular and tubulointerstitial injury after ADR-injection compared to WT [36]. In a model of FSGS due to protein overload [37], factor H (fH)-deficient mice displayed higher C3b glomerular deposition and more severe lesions than WT controls, overall supporting a pathogenic role of alternative complement activation in FSGS.

The experiments with conditional DAF removal from podocytes indicate that pathogenic complement activation occurs locally on the surface of these cells. The fact that C3aR deficiency in podocytes is also protective, indicates that C3a/C3aR interaction is the main effector mechanism responsible for the complement-induced podocyte injury. Sys-

temic administration of a C3aR antagonist prevents ADR-induced glomerulosclerosis, providing a rationale for future studies testing the hypothesis that pharmacological blockade of C3a formation or signaling downstream C3aR prevents progression of FSGS also in humans.

Importantly, our data with conditional DAF knock-out mice were replicated in male and female BALB/c mice, as well as in B6 animals that are more resistant to ADR. Previous data indicate that different susceptibility to ADR across mouse strains depends on mutations in the *Prkdc* gene, which encodes a critical nuclear DNA double-stranded break repair protein [25]. However, our data suggest that strain susceptibility to ADR could, at least in part, also depend on different predisposition to complement activation. While both BALB/c and B6 mice expressed DAF in podocytes, DAF cleavage and C3b deposition in the glomeruli were more pronounced in BALB/c animals. Overall, these data concur to document that complement activation is a central pathogenic mechanism in glomerulosclerosis affecting disease severity.

Our in vitro and in vivo data indicate that ADR promotes DAF cleavage on podocyte membranes through the upregulation of PLAD. PLAD is specific for the glycosyl-phosphatidylinositol anchor found on many eukaryotic cell surface proteins including DAF [38]. To the best of our knowledge, this is the first demonstration that PLAD is produced by human podocytes and regulates DAF expression on their surfaces. Development of small molecules with PLAD inhibitory activity may, therefore, have clinical utility in patients with FSGS [39].

Our in vitro studies show that C3a/C3aR interaction in podocytes leads to significant cell cytoskeleton rearrangements and that this is mediated by C3a-induced increase in IL-1β production that, through an autocrine and paracrine signaling, reduces nephrin expression. Though C3a has been shown to lead to increased IL-1β production in monocytes [33] and podocytes are known for their capacity to make IL-1β [31], to the best of our knowledge this is the first study reporting a link between C3a/C3aR signaling and IL-1β production in podocytes. These new mechanistic insights may contribute to explain the antiproteinuric effects of anti-IL-1β antibody treatment in individuals with amyloidosis [40, 41].

Our in vitro and in vivo data in mice are corroborated by human findings, implicating a role for complement in both murine and human FSGS. In renal biopsies from patients with FSGS, we found the C3d deposition in the glomeruli was paralleled by a reduction in DAF expression, suggesting that complement activation is at least in part mediated by a downregulation of this regulator. The association between urinary C3a or C5a and proteinuria further supports a pathogenic role for alternative pathway complement activation in the disease and the testable hypothesis that C3a represents also a biomarker for disease activity more sensitive than proteinuria. C3d deposition was associated with podocyte expression of IL-1β in individuals with FSGS.

The present data suggest a physiological role for DAF expression on podocytes as a mechanism of protection from spontaneous activation of urinary complement components and provide mechanisms for previously unexplained observations, including that C3b deposition in the glomeruli of subjects with FSGS [42] or diabetic kidney disease

(DKD) [43] correlates with poor renal survival and that subjects with loss-of-function mutations in *CD55* gene (encoding for DAF) present evidence of glomerular injury [44-46]. Intriguingly, data from the early nineties indicate that steroids, the most widely used first-line therapy for FSGS, inhibit activation of the alternative pathway of complement activation. In light of our new discoveries, this effect could, at least in part, explain the antiproteinuric effects of steroid treatment in FSGS cases.

Our study has some limitations. While the present data indicate that complement cascade is activated through the alternative pathway, we cannot discriminate between a primary activation of this pathway and an uncontrolled activation of the downstream amplification loop. Also, our studies do not decipher the source of complement factors activated in the glomeruli, i.e. whether they are produced by the liver and other organs and filtered into the kidney or produced by the kidney itself. Previous data indicate that systemic, but not kidney produced complement is the major source of complement factors activated in the glomeruli in the albumin overload model of FSGS [47]. However, we also show that in glomeruli from humans with FSGS there is an upregulation of *C3* complement gene, suggesting that the kidney represents another source of complement.

Our studies mainly focused on FSGS. However, data by others support the concept that complement activation is implicated in the pathogenesis of other glomerular diseases. Therefore, our current working model could apply to other proteinuric nephropathies.

CONCLUSIONS

In summary, our data support a conceptual paradigm shift, suggesting as fundamental the the specific role of C3a/C3aR signaling in podocytes injury in the pathogenesis of FSGS. Our data are of sure interest also for other different proteinuric nephropathies. Various inhibitors of complement component C3 and antagonists of the C3aR, along with IL-1β or IL-1R1 antagonists are actively being developed by pharmaceutical companies. Therefore, our data set the basis for future interventional trials testing the hypothesis that counteracting C3a/C3aR and/or IL-1β/IL-1R1 signaling prevents or retards progression of proteinuric nephropathies [48].

References

1. Kitiyakara C, Eggers P, Kopp JB: Twenty-one-year trend in ESRD due to focal segmental glomerulosclerosis in the United States. *Am J Kidney Dis* 2004, 44(5): 815-825.

2. Cravedi P, Kopp JB, Remuzzi G: Recent progress in the pathophysiology and treatment of FSGS recurrence. *Am J Transplant* 2013, 13(2):266-274.

3. Cravedi P, Angeletti A, Remuzzi G: New biologics in the treatment of rare glomerular diseases of childhood. *Curr Opin Pharmacol* 2017, 33:27-33.

4. Pollak MR: Inherited podocytopathies: FSGS and nephrotic syndrome from a genetic viewpoint. *J Am Soc Nephrol* 2002, 13(12):3016-3023.

5. Asano T, Niimura F, Pastan I, Fogo AB, Ichikawa I, Matsusaka T: Permanent genetic tagging of podocytes: fate of injured podocytes in a mouse model of glomerular sclerosis. *J Am Soc Nephrol* 2005, 16(8):2257-2262.

6. Matsusaka T, Xin J, Niwa S, Kobayashi K, Akatsuka A, Hashizume H, Wang QC, Pastan I, Fogo AB, Ichikawa I: Genetic engineering of glomerular sclerosis in the mouse via control of onset and severity of podocyte-specific injury. *J Am Soc Nephrol* 2005, 16(4):1013-1023.

7. Wharram BL, Goyal M, Wiggins JE, Sanden SK, Hussain S, Filipiak WE, Saunders TL, Dysko RC, Kohno K, Holzman LB *et al*: Podocyte depletion causes glomerulosclerosis: diphtheria toxin-induced podocyte depletion in rats expressing human diphtheria toxin receptor transgene. *J Am Soc Nephrol* 2005, 16(10):2941-2952.

8. Cravedi P, Heeger PS: Complement as a multifaceted modulator of kidney transplant injury. *J Clin Invest* 2014, 124(6):2348-2354.

9. Angeletti A, Reyes-Bahamonde J, Cravedi P, Campbell KN: Complement in Non-Antibody-Mediated Kidney Diseases. *Front Med (Lausanne)* 2017, 4:99.

10. Mathern DR, Heeger PS: Molecules Great and Small: The Complement System. *Clin J Am Soc Nephrol* 2015, 10(9):1636-1650.

11. Servais A, Noel LH, Roumenina LT, Le Quintrec M, Ngo S, Dragon-Durey MA, Macher MA, Zuber J, Karras A, Provot F *et al*: Acquired and genetic complement abnormalities play a critical role in dense deposit disease and other C3 glomerulopathies. *Kidney Int* 2012, 82(4):454-464.

12. Sethi S, Nester CM, Smith RJ: Membranoproliferative glomerulonephritis and C3 glomerulopathy: resolving the confusion. *Kidney Int* 2012, 81(5):434-441.

13. Smith RJH, Appel GB, Blom AM, Cook HT, D'Agati VD, Fakhouri F, Fremeaux-Bacchi V, Jozsi M, Kavanagh D, Lambris JD *et al*: C3 glomerulopathy - understanding a rare complement-driven renal disease. *Nat Rev Nephrol* 2019, 15(3):129-143.

14. Bao L, Haas M, Pippin J, Wang Y, Miwa T, Chang A, Minto AW, Petkova M, Qiao G, Song WC *et al*: Focal and segmental glomerulosclerosis induced in mice lacking de-

cay-accelerating factor in T cells. *The Journal of clinical investigation* 2009, 119(5): 1264-1274.

15. Coffelt SB, Kersten K, Doornebal CW, Weiden J, Vrijland K, Hau CS, Verstegen NJM, Ciampricotti M, Hawinkels L, Jonkers J *et al*: IL-17-producing gammadelta T cells and neutrophils conspire to promote breast cancer metastasis. *Nature* 2015, 522(7556): 345-348.

16. Ma LJ, Fogo AB: Model of robust induction of glomerulosclerosis in mice: importance of genetic background. *Kidney Int* 2003, 64(1):350-355.

17. Guo J, Ananthakrishnan R, Qu W, Lu Y, Reiniger N, Zeng S, Ma W, Rosario R, Yan SF, Ramasamy R *et al*: RAGE mediates podocyte injury in adriamycin-induced glomerulosclerosis. *J Am Soc Nephrol* 2008, 19(5):961-972.

18. Saleem MA, O'Hare MJ, Reiser J, Coward RJ, Inward CD, Farren T, Xing CY, Ni L, Mathieson PW, Mundel P: A conditionally immortalized human podocyte cell line demonstrating nephrin and podocin expression. *J Am Soc Nephrol* 2002, 13(3):630-638.

19. Da Sacco S, Lemley KV, Sedrakyan S, Zanusso I, Petrosyan A, Peti-Peterdi J, Burford J, De Filippo RE, Perin L: A novel source of cultured podocytes. *PLoS One* 2013, 8(12):e81812.

20. Karpinski J, Lajoie G, Cattran D, Fenton S, Zaltzman J, Cardella C, Cole E: Outcome of kidney transplantation from high-risk donors is determined by both structure and function. *Transplantation* 1999, 67(8):1162-1167.

21. Medof ME, Kinoshita T, Nussenzweig V: Inhibition of complement activation on the surface of cells after incorporation of decay-accelerating factor (DAF) into their membranes. *J Exp Med* 1984, 160(5):1558-1578.

22. Sakemi T, Ohtsuka N, Tomiyoshi Y, Morito F: Sex difference in progression of adriamycin-induced nephropathy in rats. *Am J Nephrol* 1996, 16(6):540-547.

23. Chen A, Sheu LF, Ho YS, Lin YF, Chou WY, Chou TC, Lee WH: Experimental focal segmental glomerulosclerosis in mice. *Nephron* 1998, 78(4):440-452.

24. Garovic VD, August P: Sex Differences and Renal Protection: Keeping in Touch with Your Feminine Side. *J Am Soc Nephrol* 2016, 27(10):2921-2924.

25. Papeta N, Zheng Z, Schon EA, Brosel S, Altintas MM, Nasr SH, Reiser J, D'Agati VD, Gharavi AG: Prkdc participates in mitochondrial genome maintenance and prevents Adriamycin-induced nephropathy in mice. *The Journal of clinical investigation* 2010, 120(11):4055-4064.

26. Breyer MD, Bottinger E, Brosius FC, 3rd, Coffman TM, Harris RC, Heilig CW, Sharma K, Amdcc: Mouse models of diabetic nephropathy. *J Am Soc Nephrol* 2005, 16(1):27-45.

27. Thurman JM, Wong M, Renner B, Frazer-Abel A, Giclas PC, Joy MS, Jalal D, Radeva MK, Gassman J, Gipson DS *et al*: Complement Activation in Patients with Focal Segmental Glomerulosclerosis. *PLoS One* 2015, 10(9):e0136558.

28. Macconi D, Abbate M, Morigi M, Angioletti S, Mister M, Buelli S, Bonomelli M, Mundel P, Endlich K, Remuzzi A *et al*: Permselective dysfunction of podocyte-podocyte contact upon angiotensin II unravels the molecular target for renoprotective intervention. *Am J Pathol* 2006, 168(4):1073-1085.

29. Da Sacco S, Sedrakyan S, Boldrin F, Giuliani S, Parnigotto P, Habibian R, Warburton D, De Filippo RE, Perin L: Human amniotic fluid as a potential new source of organ specific precursor cells for future regenerative medicine applications. *J Urol* 2010, 183(3):1193-1200.

30. Zhao L, Wang X, Sun L, Nie H, Liu X, Chen Z, Guan G: Critical role of serum response factor in podocyte epithelial-mesenchymal transition of diabetic nephropathy. *Diab Vasc Dis Res* 2016, 13(1):81-92.

31. Anders HJ: Of Inflammasomes and Alarmins: IL-1beta and IL-1alpha in Kidney Disease. *J Am Soc Nephrol* 2016, 27(9):2564-2575.

32. Yan J, Li Y, Yang H, Zhang L, Yang B, Wang M, Li Q: Interleukin-17A participates in podocyte injury by inducing IL-1beta secretion through ROS-NLRP3 inflammasome-caspase-1 pathway. *Scand J Immunol* 2018, 87(4):e12645.

33. Asgari E, Le Friec G, Yamamoto H, Perucha E, Sacks SS, Kohl J, Cook HT, Kemper C: C3a modulates IL-1beta secretion in human monocytes by regulating ATP efflux and subsequent NLRP3 inflammasome activation. *Blood* 2013, 122(20): 3473-3481.

34. Schlondorff J: Nephrin AKTs on actin: The slit diaphragm-actin cytoskeleton signaling network expands. *Kidney Int* 2008, 73(5):524-526.

35. Lenderink AM, Liegel K, Ljubanovic D, Coleman KE, Gilkeson GS, Holers VM, Thurman JM: The alternative pathway of complement is activated in the glomeruli and tubulointerstitium of mice with adriamycin nephropathy. *Am J Physiol Renal Physiol* 2007, 293(2):F555-564.

36. Turnberg D, Lewis M, Moss J, Xu Y, Botto M, Cook HT: Complement activation contributes to both glomerular and tubulointerstitial damage in adriamycin nephropathy in mice. *J Immunol* 2006, 177(6):4094-4102.

37. Morigi M, Locatelli M, Rota C, Buelli S, Corna D, Rizzo P, Abbate M, Conti D, Perico L, Longaretti L *et al*: A previously unrecognized role of C3a in proteinuric progressive nephropathy. *Sci Rep* 2016, 6:28445.

38. Davitz MA, Hom J, Schenkman S: Purification of a glycosyl-phosphatidylinositol-specific phospholipase D from human plasma. *J Biol Chem* 1989, 264(23): 13760-13764.

39. Frohman MA: The phospholipase D superfamily as therapeutic targets. *Trends Pharmacol Sci* 2015, 36(3):137-144.

40. Varan O, Kucuk H, Babaoglu H, Guven SC, Ozturk MA, Haznedaroglu S, Goker B, Tufan A: Efficacy and safety of interleukin-1 inhibitors in familial Mediterranean fever patients complicated with amyloidosis. *Mod Rheumatol* 2019, 29(2):363-366.

41. Dinarello CA, Simon A, van der Meer JW: Treating inflammation by blocking interleukin-1 in a broad spectrum of diseases. *Nat Rev Drug Discov* 2012, 11(8):633-652.

42. Liu J, Xie J, Zhang X, Tong J, Hao X, Ren H, Wang W, Chen N: Serum C3 and Renal Outcome in Patients with Primary Focal Segmental Glomerulosclerosis. *Sci Rep* 2017, 7(1):4095.

43. Bus P, Chua JS, Klessens CQF, Zandbergen M, Wolterbeek R, van Kooten C, Trouw LA, Bruijn JA, Baelde HJ: Complement Activation in Patients With Diabetic Nephropathy. *Kidney Int Rep* 2018, 3(2):302-313.

44. Kurolap A, Eshach-Adiv O, Baris HN: CD55 Deficiency and Protein-Losing Enteropathy. *N Engl J Med* 2017, 377(15):1500.

45. Ozen A, Comrie WA, Lenardo MJ: CD55 Deficiency and Protein-Losing Enteropathy. *N Engl J Med* 2017, 377(15):1499-1500.

46. Angeletti A, Marasa M, Cravedi P: CD55 Deficiency and Protein-Losing Enteropathy. *N Engl J Med* 2017, 377(15):1499.

47. Abbate M, Zoja C, Corna D, Rottoli D, Zanchi C, Azzollini N, Tomasoni S, Berlingeri S, Noris M, Morigi M *et al*: Complement-mediated dysfunction of glomerular filtration barrier accelerates progressive renal injury. *J Am Soc Nephrol* 2008, 19(6): 1158-1167.

48. Angeletti A, Cantarelli C, Petrosyan A, Andrighetto S, Budge K, D'Agati VD, Hartzell S, Malvi D, Donadei C, Thurman JM *et al*: Loss of decay-accelerating factor triggers podocyte injury and glomerulosclerosis. *J Exp Med* 2020, 217(9).